Theoretical Modelling on Vortex Dynamics in Jupiter and Saturn Atmospheres

by

Muhammad Mubashir Israr

BS, Physics, Air University, 2022

A thesis submitted in partial fulfillment of the requirements for the degree of

Master of Science in Applied Physics

AIR UNIVERSITY

2024

Theoretical Modelling on Vortex Dynamics in Jupiter and Saturn Atmospheres

by

Muhammad Mubashir Israr

A thesis submitted in partial fulfillment of the requirements for the degree of

Master of Science in Applied Physics

SUPERVISOR

Dr. Rizwan Akram

AIR UNIVERSITY

ISLAMABAD

CERTIFICATE

Department of Physics

It is hereby certified that Muhammad Mubashir Israr (222573) has successfully completed his thesis.

Dr. Rizwan Akram	**Dr. Umer Rehman**
Associate Professor	Assistant Professor
Air University	*Air University*
Supervisor	Co-Supervisor
Dr. Shakeel Mahmood	**Dr. Riaz Khan**
Associate Professor	Deputy Chief Scientist
Air University	*PTPRI*
Internal Examiner	External Examiner
Guidance and Evaluation Committee	Guidance and Evaluation Committee
Dr. Waqas khalid	**Dr. Muhammad Atif**
Professor	Professor
Air University	*Air University*
Chair Department of Physics	Dean Faculty of Basic and Applied Sciences

Prof. Dr. Zafar Ullah Koreshi

Air University

Dean Faculty of Graduate Studies

Air University

Office of Graduate Studies

Thesis Submission Checklist

This checklist should be completed at the time of submission of your thesis. One copy of this should be placed inside your thesis and one copy submitted to the Office of Graduate Studies.

Please ensure to tick all boxes.

□	Title page as in template
□	Declaration
□	Acknowledgments
□	Nomenclature (SI units, symbols and abbreviations)
□	Abstract
□	Contents
□	List of Figures
□	List of Tables
□	Figure captions
□	Table captions
□	Equations in table of three columns 10-80-10
□	References in APA 6th Edition format
□	Similarity report submitted along with thesis

Summary

Description	Response	Comments of HoD if any
Software used (MS Word, LaTex etc)		
Word count of thesis		
Number of pages of thesis		
Word count of abstract		
Number of Chapters		
Number of Figures		
Number of Tables		
Units used		
Number of References cited		
Number of books cited in references		
Total number of journal publications cited		
No. of journal publications of last five years cited		
Commercial or open-source codes used		
Total number of your journal papers cited		
Total number of your conference papers cited		

Name of Student: **M. Mubashir Israr** Degree Enrolled for: **MSAP**

Signature of Student: Date:

Signature of HoD: Date:

Received by Office of Graduate Studies: Date:

DECLARATION

I declare that all material in this thesis is my work, and that which is not my own work has been mentioned as such, and that no material from this work has previously been submitted or approved for the award of a degree by this or any other university.

Signature: _____

Author's Name: **Muhammad Mubashir Israr**

Dated: _____

It is certified that the work presented in this thesis is carried out and completed under my supervision.

Signature: _____

Supervisor's Name: **Dr. Rizwan Akram**

Associate Professor

Department of Physics

Air University, Islamabad

Dated: _____

Acknowledgments

My limitless thanks to Allah, the Ever-Magnificent for His help and blessings. This work would have never become possible, without His will. I am grateful to all who helped me in the completion of this research work especially I thank my supervisor Dr. Rizwan Akram and co-supervisor Dr. Umer Rehman, who has been always generous during all phases of the research. My gratitude is also toward Chairman Department Dr. Waqas Khalid for helping me in various tasks during my educational work. I am thankful to my university giving me an opportunity to complete this work. My wholehearted thanks to my family for their generous support that they provided me throughout my life and particularly during the process of pursuing this degree. Special thanks to my parents for their unconditional love and prayers. Thanks to all my friends, who have been very supportive during this work. I am very appreciative to my research fellows who participated in this study. Also, deepest thanks go to all supporting staff who took part in making this thesis a reality.

Thank you All

Theoretical Modelling on Vortex Dynamics in Jupiter and Saturn Atmospheres

by

Muhammad Mubashir Israr

BS, Physics, Air University, 2022

Submitted in partial fulfillment of the requirements for the degree of

Master of Science in Physics, Air University

Abstract

Focus of this research is to model a theoretical frame work that explains the dynamics of vortices occurring in Jupiter and Saturn atmosphere, that are stable and long lasting. Based on data from the WFC3/UVIS instrument on board the Hubble Space Telescope (HST), we presented a theory describing the dynamics of vortices in Jupiter and Saturn atmosphere. The charged dust cloud and neutrals with background of un-bounded plasma is used as a modelling tool for driven-dissipative complex flow systems in nature. We predicted structural variations of self-organized vortices in giant planes atmosphere, such as the GRS and White Ovals. The steady state flow linear and nonlinear solutions are obtained using a 2D hydrodynamic model. The steady driven dust circulation of the vortices in giant planet atmosphere are revealed by these linear and nonlinear solutions. Inner structural changes connected to driving fields rather than kinematic viscosity, it is demonstrated that high-speed collar rings that are persistent around the uniform vorticities of the GRS. This analysis also illuminates the role played by the driving field, boundaries, and Jovian parameter in establishing the typical size, circulation direction, strength, and drift of the vortices in atmosphere of giant planet.

Thesis Supervisor: Dr. Rizwan Akram

Title: Associate Professor of Physics

Table of Contents

List of Figure

List of Tables

Symbols and Abbreviations

English upper case

H	Atmospheric height
L_o	Zonal Characteristic Length
Lx	Zonal length scale
L_y	Meridionl length scale
R_0	Rossby number
U_0	Zonal Velocity
U	Velocity in x direction
V	Velocity in y direction

English lower case

b	Body forces
f	Coriolis parameter
g	Gravity
kx, ky	Wavenumbers
u	Local flow velocity

Greek upper case

ψ	Stream function
∇	Nabla operator
Ω	Angular rotation velocity

Greek lower case

β	Constant for coordinate origin
γ	Electrostatic parameter
ϕ	Electric potential
σ	Stress tensor
ρ	Density
μ	Kinematic viscosity
ω	Angular frequency

Chapter 1: Introduction

1.1 Solar System

The solar system comprises eight planets, dwarf planets, moons, asteroids, comets, and dust bound by gravity. Our cosmic neighborhood is it. All other celestial bodies revolve around the sun, which is located at their core.

The major elements that make up our solar system are outlined below.

Sun: The Sun is a massive ball of heated plasma that illuminates and warms the solar system. This star generates energy by converting hydrogen into helium through nuclear fusion.

Planets: In our solar system, there are eight known planets that are typically divided into two groups:

1.2 Inner Planets:

These four planets are rocky and relatively close to the Sun. They are, in order of increasing distance from the Sun:

Mercury: The planet that is nearest to the Sun and the smallest in our solar system is called Mercury. This is a rocky globe, the dayside seared by the tremendous heat of the Sun, the night side sunk into freezing darkness.

Venus: Our nearest planetary neighbor, Venus, is a fascinating planet covered in a dense, poisonous atmosphere. Venus is far from friendly, despite being referred to as Earth's twin because of similarities in mass and size. Its surface is hot enough to melt lead, making it the hottest planet in our solar system.

Earth: The only planet in our solar system that is known to sustain life as we know it is Earth, our home planet, which is located third from the Sun. There's a stunning blue stone floating in a huge void of space. Several vortices have been observed on earth but these vortices has very short life span. On the other hand vortices on giants planets are long lasting and these vortices have stable shape and remain there for more than hundred years.

Mars: Mars, approximately five times the distance from the Sun compared to Earth, is a rocky, icy planet. The atmosphere is relatively thin. Mars, known as the "Red Planet" because of its iron oxide-covered surface, captivates human interest for generations.

1.3 Outer Planets:

These four planets exhibit larger sizes and greater distances from the Sun. The atmospheres of these gas giants consist mainly of hydrogen and helium.

The four planets, located beyond the asteroid belt, are referred to as outer planets. These gas giants are significantly larger and more massive, primarily consisting of hydrogen and helium. The text provides a classification breakdown.

1.4 Gas Giants (Jovian Planets):

Jupiter: Jupiter, the largest planet in the solar system, hosts the Great Red Spot, an immense anticyclone storm, and a swirling atmosphere. The magnificent gas giant Jupiter, the dominating planet in our solar system, spins with brilliant clouds and an enduring storm.

Saturn: With a well-known ring system of rock and ice, Saturn stands as the second-largest planet in the solar system. Saturn, the second largest planet in our solar system, is six planets away from the Sun. Known for its stunning ring system, this gas giant consists of billions of ice and rock particles.

Uranus: A tilted ice giant orbits as a pale blue planet. Ice giant Uranus, positioned sixth from the Sun, differs from other solar system planets. With a peculiar tilt and an aura of surprisingly vivid blue, it's an intriguing and unusual place.

Neptune: The deep blue, gas giant farthest from the Sun boasts supersonic winds. The eighth and farthest planet from the Sun, Neptune, boasts supersonic winds and a deep blue atmosphere. In this world, icy temperatures and powerful storms prevail. These planets possess a gas composition mainly of hydrogen and helium, with slight quantities of methane, ammonia, and water vapor. **Structure:** Not a solid surface, but a dense atmosphere that becomes liquid and then solid as pressure builds up toward the center. **Rings:** Although Saturn's ring system is the most noticeable,

all four gas giants contain them. Billionths of particles, ranging from dust grains to massive stones that orbit the planet, make up these rings. **Great Storms:** While the Great Red Spot on Jupiter is a well-known example, massive anticyclone storms that can last for decades can be seen on all the gas giants. **Moons:** There are numerous moons orbiting the gas giants, ranging in size from tiny, stony moons to massive moons larger than certain planets. Mercury is smaller than Ganymede, the moon of Jupiter. Because Uranus and Neptune contain a larger percentage of elements heavier than hydrogen and helium, like oxygen, carbon, and nitrogen, than Jupiter and Saturn, it's vital to note that they are frequently referred to as ice giants to separate them from those planets [1]. Given the lower temperatures in the outer solar system, these elements are probably frozen as ice.

1.5 Terrestrial Planets vs Giant Planets

1.5.1 Terrestrial Planets

Location: Found in the inner solar system, closer to the Sun. These include: Mercury, Venus, Earth, and Mars. **Composition:** Primarily made up of rock and metal, with a solid, rocky surface. **Size:** Smaller and less massive than giant planets. **Atmosphere:** Less massive atmospheres than big planets, primarily made up of carbon dioxide (Mars), nitrogen/oxygen (Earth), or carbon dioxide (Venus). **Magnetic Field:** Weaker magnetic fields compared to giant planets. **Internal Structure:** Typically have a central core of iron, a surrounding mantle of rock, and sometimes a crust made of lighter elements. **Moons:** Generally have few or no moons (Earth has one, Mars has two).

1.5.2 Giant Planets

In the outer solar system, the location is more distant from the Sun. Uranus, Neptune, Jupiter, and Saturn, being primarily composed of hydrogen and helium gas, also contain trace amounts of methane, ammonia, and water vapor. These planets are significantly larger and more massive than their terrestrial counterparts. Thick and extensive atmospheres, predominantly constituted of hydrogen and helium. Strong magnetic fields are generated within planets due to the movement of electrically charged particles in their liquid metallic interiors. Moons exhibit varying sizes, from small, rocky bodies to large ones that dwarf some planets, all orbiting around planets with no

discernible solid surface, only an atmosphere that thickens into a liquid and eventually solidifies as pressure increases towards the center.

1.6 Gas Giants vs Ice Giants

1.6.1 Gas Giants

Jupiter and Saturn, being the largest planets in our solar system, are recognized as gas giants. Mostly composed of hydrogen and helium, trace amounts of methane, ammonia, and water vapor are present. Instead of a solid core, they have a deep atmosphere that transitions under pressure from a liquid state to a solid form at their center. Huge ring systems consisting of billions of particles, from dust grains to massive boulders, are present in all four gas giants. The Great Red Spot on Jupiter is the most well-known example of the massive, protracted anticyclone storms that are characteristic of the gas giants. The giants have numerous moons, some of which are surprisingly large. For instance, Jupiter's moon Ganymede is bigger than Mercury.

1.6.2 Ice Giants

Neptune and Uranus are examples of ice giants. Although ice giants and gas giants have similar abundances of hydrogen and helium in their atmospheres, ice giants have larger concentrations of heavier elements such as oxygen, carbon, and nitrogen. The cold temperatures of the outer solar system are thought to have frozen these heavier elements into ices. Because of the heavier elements in their composition, ice giants are denser than gas giants. Their interior structure, which has a thick atmosphere that transitions to a liquid and solid core, is comparable to that of gas giants. Ice giants have smaller, fainter ring systems than gas giants, which are more noticeable. Even though they are often smaller than those giants of ice, ice also has a lot of moons. Ice giants atmosphere is consist of gases other than hydrogen and helium gases, as these two are light molecular weight gases while other gases present on ice giants are heavier in their molecular weight. So that’s why these planets are named as ice giants because of their atmospheric composition of heavier gases than hydrogen and helium. These two planets comes in outer planets while other two planets like Jupiter and Saturn are named as gas giants because of atmospheric composition of heavier gases that include hydrogen and helium gases. Small traces of other gases like ammonia and methane is also present on these planets.

Table 1-1 : Gas Giants vs Ice Giants

Feature	**Gas Giants**	**Ice Giants**
Composition	Mostly hydrogen and helium, with some methane, ammonia, and water vapor	Higher proportion of heavier elements (oxygen, carbon, nitrogen) than gas giants
Density	Lower density	Higher density
Rings	Prominent and extensive ring systems	Fainter and less extensive ring systems
Examples	Jupiter, Saturn	Uranus, Neptune

1.7 Overview of Vortex

A vortex denotes the region in a fluid where the flow revolves around a central axis. Vortices are influenced by viscosity, the Coriolis force, electric fields, and drag forces. Vortices in gas giant atmospheres like Jupiter and Saturn are the primary focus of this extensive study.

Vortices in Jupiter and Saturn's atmospheres result from a complex interplay of forces. Understanding these dynamics sheds light on atmospheric behaviors of extraterrestrial bodies and advances fluid mechanics research.

1.7.1 Vortex Dynamics

Vortices emerge when fluid flow is disrupted, causing rotation. The cause could be any combination of differential heating, pressure changes, or multiple fluid interactions. Frequently on Jupiter and Saturn, the formation of vortices is caused by turbulent fluxes in the atmosphere, resulting from variations in pressure and temperature.

Rotation and Structure:

A vortex consists of a central core with maximum rotation intensity, surrounded by a progressively weaker swirling flow. A vortex's stability is influenced by the balance of forces acting upon it, as exemplified by Jupiter's Great Red Spot. So in general we can say that in the core of vortex, vorticity is high.

1.7.2 Forces Affecting Vortices

Viscosity:

A fluid's internal friction is expressed through its viscosity. The Great Red Spot on Jupiter, a feature that's persisted for centuries, shows that lower viscosity keeps vortices stable and energetic for long durations. Vortices lose strength and eventually dissipate due to increased viscosity causing more energy loss.

Coriolis force:

Vortices form due to the Coriolis force generated by the earth's rotation. At higher latitudes, the force is stronger. The Coriolis force maintains Jupiter and Saturn's massive, stable vortices by counteracting the outward centrifugal forces and inward pressure gradients.

Electric Forces and Fields:

Electric forces on charged particles in a vortex can impact cloud dynamics and lightning. These forces can change the vortices' stability and structure by altering the atmosphere's microphysics.

Drag Forces:

Drag forces originate from the resistance encountered by the moving fluid. They aid in the dissipation of kinetic energy, thereby influencing the duration and form of vortices. The boundary layers exhibit significant drag due to shear and turbulence induced by the vortex's interaction with the fluid.

1.7.3 Specific Examples on Jupiter and Saturn

Jupiter’s Great Red Spot:

The Great Red Spot, a longstanding anticyclone storm, has existed for over 400 years. Its longevity results from a combination of Coriolis forces, low atmospheric viscosity, and interactions with nearby zonal jets. So it is an anticyclone vortex with shape that is well define.

Saturn’s Hexagon:

A hexagonal vortex structure, possibly resulting from Saturn's rotation and atmospheric waves, is located at its north pole. This hexagon's complex interplay of forces forms long-lasting, stable vortices.

Smaller Vortices:

Numerous smaller vortices can merge, split, or be absorbed by bigger systems. These smaller vortices are more directly influenced by local atmospheric conditions and form, interact, and evaporate over shorter durations on both Jupiter and Saturn.

1.8 Jupiter

Jupiter is the fifth-from-the-Sun planet in the solar system and it is most massive. It is among the brightest celestial bodies in the night sky, outperformed only by the Moon, Venus, and occasionally Mars.

Without knowing the planet's actual size, ancient astronomers named Jupiter after the Roman king of the gods and sky, sometimes known as Jove. The name is fitting, since Jupiter is larger than all the other planets put together. With even a modest telescope, one can observe the colorful cloud bands of the Sun, which rotates more than twice as quickly as Earth every ten hours. The Sun takes roughly 12 Earth years to orbit. It has 92 known moons and a small ring system. Under its frozen surface, Jupiter's moon Europa may be concealing a warm ocean and perhaps even life of some sort, according to some astronomers. So in Jupiter atmosphere we see that there are several activities happening but, we do not know about their actual dynamics. As vortex present there are long lasting and stable but as these have high energy so why they are long lasting. To find out its answer many researchers have given their point of view that there might be some internal reactions going on in the core of the vortex or Jupiter atmosphere may be receiving light directly from sun. Still we are unable to find out exact reason behind these long lasting vortices. Modest telescope, one can observe the colorful cloud bands of the Sun, which rotates more than twice as quickly as Earth every ten hours. The Sun takes roughly 12 Earth years to orbit. So in Jupiter atmosphere we see that there are several activities happening but we do not know about their actual dynamics.

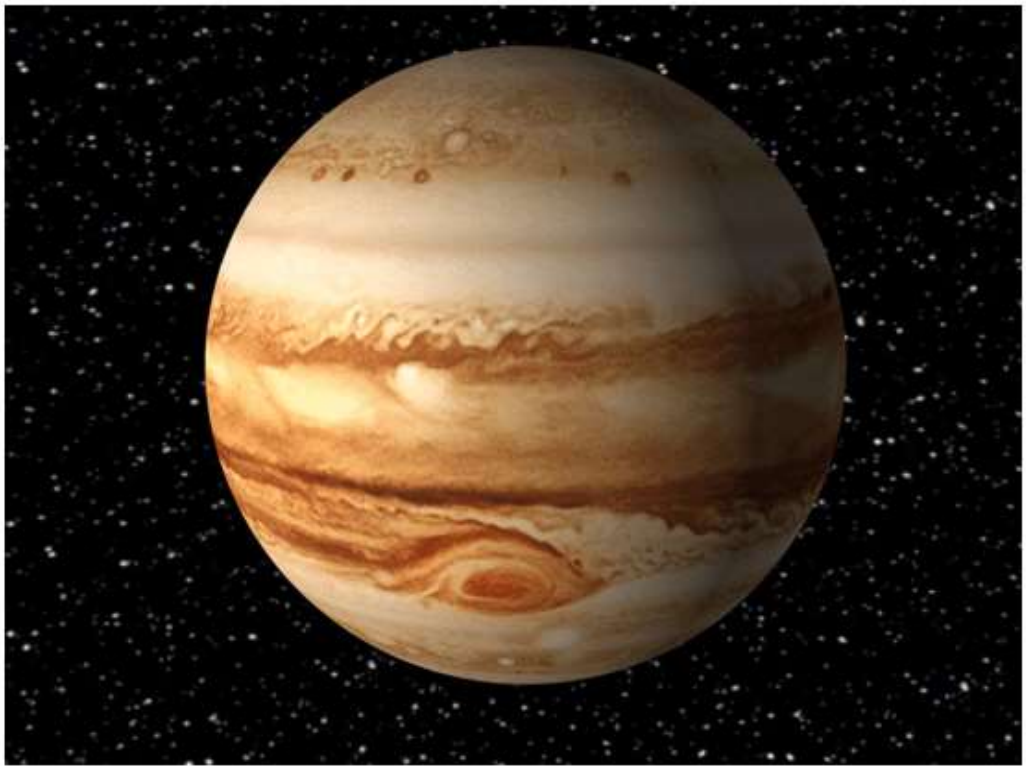

Figure 1.1 : Jupiter [1]

Jupiter produces more energy than it takes from the Sun because it has an internal heat source. Its deep interior is under such extreme pressure that hydrogen is present there in a flowing metallic state. With a magnetosphere so massive that, if it could be viewed from Earth, its apparent diameter would surpass that of the Moon, this giant has the strongest magnetic field of any planet. Intense radio noise bursts are also produced by Jupiter's system, which sporadically emits more energy than the Sun at certain frequencies. Jupiter, for all its superlatives, is essentially composed of just two elements: hydrogen and helium, and its average density is hardly higher than that of water. With a magnetosphere so massive that, if it could be viewed from Earth, its apparent diameter would surpass that of the Moon, this giant has the strongest magnetic field of any planet. Intense radio noise bursts are also produced by Jupiter's system, which sporadically emits more energy than the Sun at certain frequencies. The Gaseous Nature of Jupiter: Jupiter's lower atmosphere, where the storm starts.

Table 1-2 : Planetry data of Jupiter

Mean distance from Sun	778,340,821 km (5.2 AU)
Eccentricity of orbit	0.048
Inclination of orbit to ecliptic	1.3°
Jovian year (sidereal period of revolution)	11.86 Earth years
Visual magnitude at mean opposition	−2.70
Mean synodic perio	398.88 Earth days
Mean orbital velocity	13.1 km/sec
Equatorial radius	71,492 km
Polar radius	66,854 km
Mass	18.98×10^{26} kg
Mean density	1.33 g/cm^3
Gravity	2,479 cm/sec^2
Escape velocity	60.2 km/sec
System I (±10° from equator)	9 hr 50 min 30 sec
System II (higher latitudes)	9 hr 55 min 41 sec
System III (magnetic field)	9 hr 55 min 29 sec
Inclination of equator to orbit	3.1°
Dimensions of Great Red Spot	20,000 × 12,000 km
Magnetic field strength at equator	4.3 gauss
Number of known moons	66
Planetary ring system	1 main ring; 3 less-dense components

1.8.1 Jupiter's Great Red Spot: A Swirling Mystery

With winds reaching up to 200 mph, the largest and strongest hurricanes ever seen on Earth measured more than 1,000 miles in diameter. Its width allows it to cross almost every state in the union east of Texas. But the Great Red Spot, a massive storm on Jupiter, dwarfs even that type of storm. Big there refers to anything twice as wide as Earth. The Great Red Spot has been whirling madly across Jupiter's skies for the past 150 years—possibly even longer—with turbulent winds

that can reach speeds of up to 400 mph. Even while humans began using telescopes to see Jupiter in the 1600s and noticed a large patch there, it is still unknown if these observations were made of a distinct storm. Scientists continue to struggle to understand what causes the Great Red Spot's swirl of reddish hues, even though they are aware that it exists and has for some time.

The reason behind the color of Jupiter's Great Red Spot is still a mystery to scientists. This is the reason why:

The Gaseous Nature of Jupiter: Jupiter's lower atmosphere, where the storm starts, is challenging to analyze because of its immense size and absence of solid ground. Restricted Observations: Only the high clouds may be observed by spacecraft and telescopes, making a full image impossible. Knowing more about the Great Red Spot could advance our understanding of: The Weather Systems of Earth: Though on a grander scale, the same physical processes govern Jupiter's weather. Exoplanet Atmospheres: Researching Jupiter Aids in Understanding Planets outside Our Solar System's Atmospheres.

Challenges in Solving the Mystery:

Chemical Composition Uncertainty: The way that compounds like ammonia and ammonium hydrosulfide interact and produce color in Jupiter's atmosphere is a mystery to scientists. Restricted Function of Identified Substances: The atmosphere is mostly composed of these compounds that give things their color.

Current Research Efforts:

Simulating Chemical Reactions: In order to determine whether ammonium hydrosulfide causes the red color seen on Jupiter, scientists are subjecting it to charged particle bombardment in lab settings, such as cosmic rays. Examining Different Hypotheses: Although ammonium hydrosulfide is the most likely culprit, the red hue could also be caused by other substances alone or in combination. With winds reaching up to 200 mph, the largest and strongest hurricanes ever seen on Earth measured more than 1,000 miles in diameter. Its width allows it to cross almost every state in the union east of Texas. So many researcher are doing work on vortices but still we are unable to find out there dynamics.

The Road Ahead:

Further intricate lab tests that replicate Jupiter's atmosphere's temperature, radiation exposure, and light exposure are needed to solve the enigma.

1.8.2 Atmosphere of Jupiter

The clouds and the Great Red Spot

On Jupiter, a small telescope can display a great deal of detail. Multiple distinct cloud types are found in the area of the planet's atmosphere that is observable from Earth, and they are divided both horizontally and vertically. These cloud systems are subject to short-term fluctuations, but for decades they have been stable due to an underlying pattern of latitudinal currents. The planet's appearance is now commonly described using a consistent nomenclature for its alternating brilliant and dark bands, known as zones and belts, respectively. However, it appears that the underlying currents are more persistent than this pattern. Thus, the Great Red Spot seems to be a massive anticyclone, a vortex or eddy whose diameter is probably accompanied by a great depth that permits the feature to extend both well below and well beyond the primary layers of clouds. Jupiter's upper atmosphere is hundreds of degrees hotter than would be predicted from solar heating alone because of the Red Spot [2]. The atmosphere of Jupiter has distinct heights at which its clouds originate. With cloud-top temperatures of roughly 120 kelvins (K; -240 °F or -150 °C), the white clouds are the highest, with the exception of the summit of the Great Red Spot. These white clouds resemble the water-ice cirrus clouds found in Earth's atmosphere because they are made of frozen ammonia crystals. Lower levels are when the tawny clouds that are widely scattered around the world occur. They seem to originate at about 200 K (−100 °F, −70 °C), which implies that their color may be due to other ammonia-sulfur compounds such ammonium polysulfide and that they most likely consist of condensed ammonium hydrosulfide. Since hydrogen sulfide is noticeably lacking from Jupiter's atmosphere above the clouds and sulfur is very common in the universe, sulfur compounds are suggested as the likely coloring agents. Thus, the Great Red Spot seems to be a massive anticyclone, a vortex or eddy whose diameter is probably accompanied by a great depth that permits the feature to extend both well below and well beyond the primary layers of clouds. Jupiter's upper atmosphere is hundreds of degrees hotter than would be predicted from solar heating alone because of the Red Spot.

Figure 1.2 : Great red spot [2]

Many elliptical characteristics resembling Earth's cyclonic and anticyclone storm systems can be seen in the close-up photos of Jupiter that spacecraft have sent back to Earth. Every one of these systems is in motion, changing in appearance and duration according to their sizes and placements. The pastel hues of different colors seen in the cloud layers have also been shown to fluctuate; these range from the well-known salmon-colored Great Red Spot, Jupiter's largest, most noticeable, and longest-lasting feature, to browns and blue-grays, which appear to characterize the main layer's tawny yellow tint. There is no doubt that the vertical and horizontal separation of the cloud systems is accompanied by chemical variances in cloud composition, which astronomers believe to be the source of the color variations.

Jupiter lacks topographic features due to its lack of a solid surface, and latitudinal currents are the main force behind the planet's large-scale circulation. The endurance of these currents and the cloud patterns they are connected with are all the more astonishing because there isn't a solid surface with physical limits and distinct regions with differing heat capacities. So that’s may be one of the reason of stable vortices.

1.8.3 Nature of Great Red Spot

Even after rigorous observations from the Voyager, Galileo, and Juno spacecraft, the true nature of Jupiter's distinctive Great Red Spot remained a mystery at the beginning of the twenty-first century. The Great Red Spot has been constantly spotted since 1878 and may even be the same storm that was observed from 1665 to 1713 on a planet where cloud patterns have lifetimes frequently measured in days. The spot has been diminishing since the late 19th century, when it reached its greatest extent of roughly 48,000 km (30,000 miles). Since 2012, the spot, which was formerly clearly oval, has grown more circular and has shrunk at an accelerated rate of 900 km (580 miles) per year. At 16,350 km (10,159 mi) in width, it is currently large enough to fit Earth comfortably. The feature's durability and possibly its unique color can be attributed to these enormous proportions.

Thus, the Great Red Spot seems to be a massive anticyclone, a vortex or eddy whose diameter is probably accompanied by a great depth that permits the feature to extend both well below and well beyond the primary layers of clouds. Jupiter's upper atmosphere is hundreds of degrees hotter than would be predicted from solar heating alone because of the Red Spot, which is heating the planet from below. The lower extension of the spot needs to be monitored.

1.8.4 Cloud Composition

The atmosphere of Jupiter has distinct heights at which its clouds originate. With cloud-top temperatures of roughly 120 kelvins (K; -240 °F or -150 °C), the white clouds are the highest, with the exception of the summit of the Great Red Spot. These white clouds resemble the water-ice cirrus clouds found in Earth's atmosphere because they are made of frozen ammonia crystals. Lower levels are when the tawny clouds that are widely scattered around the world occur. They seem to originate at about 200 K (−100 °F, −70 °C), which implies that their color may be due to other ammonia-sulfur compounds such ammonium polysulfide and that they most likely consist of condensed ammonium hydrosulfide. Since hydrogen sulfide is noticeably lacking from Jupiter's atmosphere above the clouds and sulfur is very common in the universe, sulfur compounds are suggested as the likely coloring agents.

Helium and hydrogen make up the majority of Jupiter's composition. All of the plentiful chemically active elements are projected to mix with hydrogen under equilibrium conditions,

which allow all of the elements present to react with one another at a temperature average for the visible portion of the Jovian atmosphere. So, it was assumed that there would be hydrogen sulfide, water, ammonia, and methane. All of these chemicals, with the exception of hydrogen sulfide, have been discovered through spectroscopic studies from Earth.

The dark brown hue of the ammonia clouds observed at even lower levels, when the recorded temperature is 260 K (8 °F, −13 °C), has also been attributed to sulfur compounds. Through what appear to be holes in the generally common tawny clouds, these clouds are seen. Consistent with their greater temperatures, they appear brilliant in images of Jupiter created from its thermal radiation recorded at a wavelength of five micrometers.

Red phosphorus, another sulfur chemical, or complex organic compounds have all been suggested as the source of the Great Red Spot's color. These theories are supported by laboratory experiments; yet, there are arguments against each of them. Near the planet's equator, dark regions can be seen close to the heads of white plume clouds, where temperatures as high as 300 K (80 °F, 27 °C) have been recorded. These so-called hot patches are reddish-tinted while looking blue-gray. They have a blue color (from sunlight's Rayleigh scattering) covered in a thin layer of reddish material. They appear to be cloud-free zones, which explains how one can "see" into them to large depths and measure high temperatures.

Table 1-3 : Atmospheric abundances for Jupiter

Gas	**Percent**
Hydrogen (H_2)	86.4
Helium (He)	13.56
Water (H_2O)	> 0.026
Methane (CH_4)	0.21
Ammonia (NH_3)	0.07
Hydrogen sulfide (H_2S)	0.007
Hydrogen deuteride (HD)	0.004
Neon (Ne)	0.002
Argon (Ar)	0.002

1.8.5 Temperature and Pressure

With instruments to detect pressure and temperature, the Galileo probe descended into Jupiter's atmosphere. It's interesting to note that pressures marginally higher than Earth's sea level pressure were associated with temperatures over the freezing point of water (273 K, 32 °F, 0 °C). The primary cause of this phenomenon is Jupiter's internal heat source, although the atmosphere's ability to trap infrared radiation also contributes to some warming, much like Earth's greenhouse effect does.

Since temperature normally decreases with altitude, the increase in temperature that happens above the tropopause is referred to as an inversion. At high altitudes, gasses and aerosol particles absorb solar radiation, causing an inversion. The atmosphere of Earth has a comparable inversion due to the existence of ozone.

1.8.6 Jupiter’s Interior

Comparable to the skin of an apple, Jupiter's atmosphere is only a small portion of the planet. The inability to directly detect anything beneath Jupiter's atmosphere forces scientists to investigate the planet's innards through indirect means.

Here's what we know based on observations:

Temperature, pressure, mass, radius, form, rotation, thermal balance, and the impact of Jupiter's gravity on satellites and moons. Jupiter has a small equator bulge and is not exactly spherical. Problems with examining Jupiter's interior: lack of information about the behavior of hydrogen and helium in conditions of tremendous heat and pressure, such as Jupiter's core. Its core is thought to be tremendously hot—roughly 25,000 Kelvin—and extremely pressurized—millions of times more than Earth's atmosphere. According to scientist there might be some reactions going inside Jupiter core that is providing heat to Jupiter vortex, and according to some of them Jupiter might be receiving energy directly from sun but there is no direct evidence of these findings. So that’s why we are looking for a comprehensive theoretical model that explain the dynamics of great red spot and other vortices.

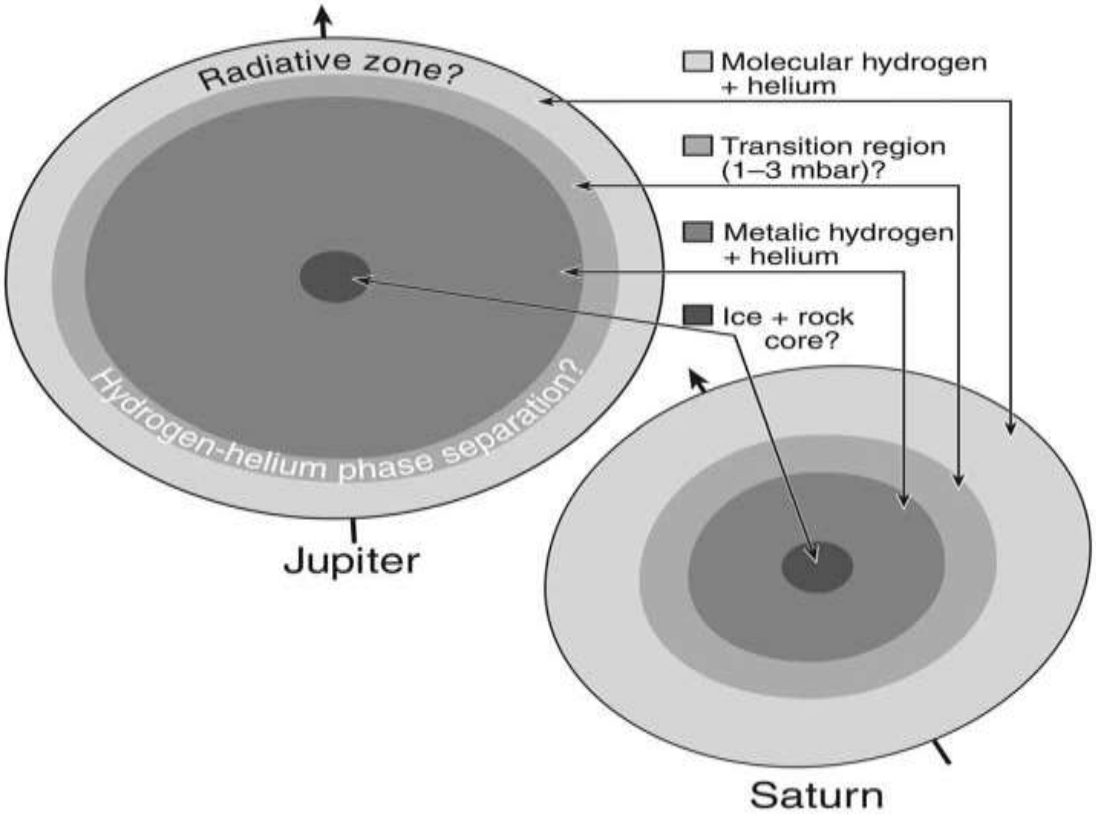

Figure 1.3 : Interior structure [3]

Key findings about Jupiter's interior:

Hydrogen cannot make up the entirety of Jupiter since that would be too big. Jupiter is probably composed of at least 70% hydrogen. It is possible that some helium has sunk towards the core of Jupiter because the amount of helium in its atmosphere is lower than predicted. Jupiter's cooling may be causing this process to continue. Hydrogen most likely changes from a molecular to a metallic form (electrons are no longer bonded to atoms) about 25% of the way below the surface. This is a shift in electrical characteristics rather than a change from liquid to solid. There's no solid surface, yet the majority of models point to a dense core. Heat emitted from helium precipitation in the core of Jupiter and residual heat from formation are most likely the sources of Jupiter's interior heat. . According to scientist there might be some reactions going inside Jupiter core that is providing heat to Jupiter vortex, and according to some of them Jupiter might be receiving energy directly from sun but there is no direct evidence of these findings. So that’s why we are looking for a comprehensive theoretical model that explain the dynamics of great red spot.

1.8.7 Hubble Captures New Images of Jupiter's Active Atmosphere

The Hubble Space Telescope has captured fresh images of Jupiter, showcasing the gas giant's ever-changing weather patterns. These observations are part of the ongoing Outer Planet Atmospheres Legacy (OPAL) program.

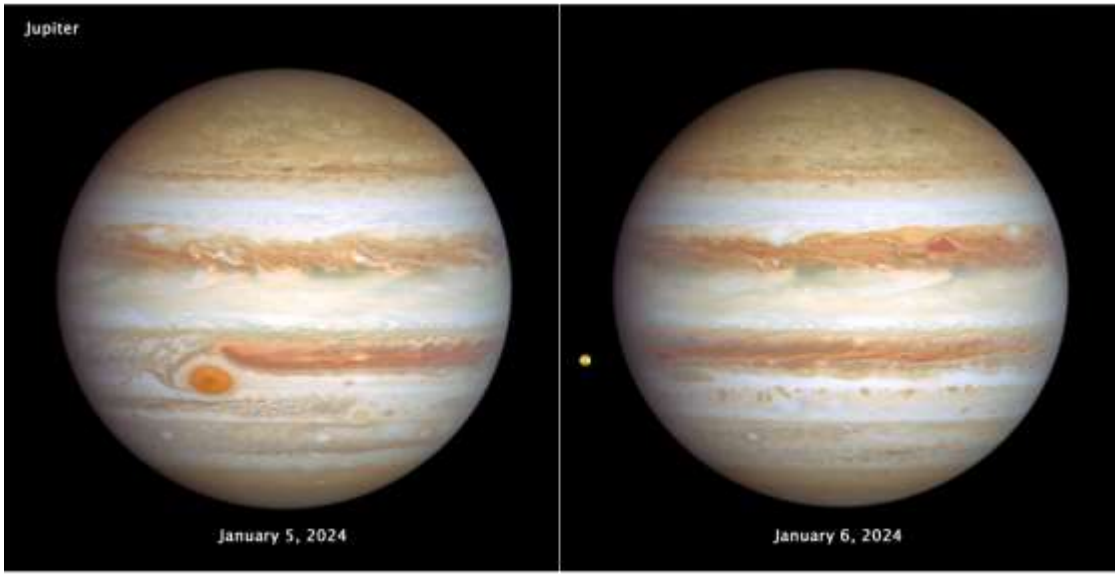

Figure 1.4 : Hubble Space Telescope imaged both sides of Jupiter [4]

Key findings:

Great Red Spot: The well-known storm is still visible, and a "Red Spot Jr." adjacent is reddish-colored again. Stormy Activity: In the southern hemisphere, two red cyclones and a reddish anticyclone are observed interacting; it is possible that their opposing rotations resist one another. Volcanic Activity on Io: Hubble has provided information about the surface features and volcanic deposits of the visible volcanic moon Io. These photos demonstrate how dynamic Jupiter's atmosphere is and how Io's continuous volcanic activity. From these observations we can find out that up to what extant Jupiter vortices has change their shape and other parameters like vorticity and wind speed.

1.9 Saturn

Saturn is the second largest planet in our solar system and is located six planets from the Sun. With its brilliant system of ice rings, Saturn stands out from the other planets.

While there are rings on other planets, none are as remarkable or intricate as those on Saturn. Similar to Jupiter, Saturn is a huge sphere primarily composed of hydrogen and helium. Saturn is the planet that has been known since ancient times and is the furthest from Earth that has been found by unaided human sight. The Roman god of agriculture and prosperity, Jupiter's father, is honored in the planet's name. Originating from the Greek deity Cronus, one of the Titans and the father of Zeus (the Roman god Jupiter), the name Saturn is derived from the Roman god of agriculture. In addition to being the planet that ancient astronomers knew to be the furthest away, Saturn was also thought to move the slowest.

Figure 1.5 : Saturn [5]

1.9.1 Atmosphere of Saturn

From Earth, Saturn looks vaguely yellow-brown. Using telescopes, scientists may see a complicated cloud system that resembles Jupiter but is less active, with red, brown, white, bands, and eddies. There are mostly molecules of helium and hydrogen (18–25% by mass) in the mixture.

Helium is less abundant than it is in the Sun; this could be because it has settled in Saturn's outer layers. Water, hydrogen sulfide, ammonia, and methane traces. Small amounts of germane, carbon monoxide, and phosphine were found; these substances were probably generated deep in the atmosphere.

1.9.2 Dynamics involved in Saturn

Zonal Winds: Saturn features east-west winds with alternating bands of light and dark clouds, just like Jupiter. Near the equator, Saturn's bands are broader and fainter. In the vicinity of the equator, wind speeds can approach 1700 km/h (1050 mph), which is far faster than on Earth. With stronger eastward jets at some latitudes and lesser westward jets in between, the winds are symmetrical around the equator. It is unknown what mechanism keeps these jets going despite atmospheric friction.

Polar Vortices: At the poles of Saturn, massive storms resembling hurricanes occur. Towering clouds and a warm eye spanning 2000 km (1200 miles) characterize the south polar vortex. These hurricanes don't have an ocean beneath them like those on Earth do.

Hexagonal Pattern: The north polar vortex is surrounded by a distinctive hexagon-shaped cloud pattern, with winds moving at a speed of 100 m/s (360 km/h) counterclockwise. Similar patterns are observed in rotating fluids, and it is unclear why it is stable and located at this particular latitude.

Smaller Features: The atmosphere of Saturn has a number of additional fascinating features, including: A "string of pearls" is a northern latitude where there are bright patches in the clouds. strong lightning storms linked to swift westward winds in the southern hemisphere.

General Organization: Wind patterns' north-south symmetry points to a more profound relationship within the globe. The reported zonal jets on Saturn may be the result of coaxial cylinders revolving at different rates, according to theoretical theories.

The north polar vortex is surrounded by a distinctive hexagon-shaped cloud pattern, with winds moving at a speed of 100 m/s (360 km/h) counterclockwise. Similar patterns are observed in rotating fluids, and it is unclear why it is stable and located at this particular latitude.

1.9.3 The Interior of Saturn

Composition: mostly hydrogen, which, under pressure, changes into a liquid condition at depth. At about one-third of the way below the clouds, hydrogen transforms into metallic hydrogen, which resembles molten metal. Denser than pure hydrogen, the central region most likely contains: Helium that has settled from the outer layers. Denser material up to 30 times the mass of Earth, possibly made of rock and ice. a rock and ice core that weighs between 15 and 18 Earth masses.

Energy Source: Given that it emits twice as much energy as it takes in from the Sun, Saturn may have an internal heat source. Most likely, a mix of the following causes this heat: Early creation heat (less likely because of Saturn's smaller mass). Helium rain precipitating into the metallic hydrogen layer. The potential energy of sinking helium droplets is converted to heat.

1.9.4 The Ring System

Overall Structure: Countless particles ranging in size from centimeters to meters make up this enormous and incredibly thin structure. It includes the faint outer rings, spanning over 16 million kilometers. Resides in the Roche limit, where tidal forces permit the existence of tiny particles but prohibit the construction of huge moons.

Composition: Mostly water ice with some darker impurities. Grains the size of dust are seen in some areas. Constant loss of ring material by impacts and interactions with Saturn's ionosphere.

Age: Based on estimates, the system may be between 10 and 100 million years old.

Possible Causes: Ice moons like as Dione or Tethys, or the fragmentation of a comet.

Principal Rings: The innermost C ring is flimsy and fragile. The brightest, thickest, and broadest is the B Ring (middle). Divided by the Cassini Division from A Ring. An outside ring: One that reaches past the Cassini Division.

Cassini Division is the most noticeable space between the B and A rings. Additional gaps generated by: Moons within the gap's gravitational pull (e.g., Pan moon and Encke gap). Moon-ring particle orbital resonances (such as the 2:1 resonance with Mimas near the Cassini Division border).

Additional Rings: Outside of the A ring is the narrow F ring. G Ring: A tumultuous ring located beyond the F ring, home to the moon Aegean. E Ring: The ring, which is quite wide and diffuse, is caused by the geysers on the moon Enceladus. Phoebe Ring: A large, thin ring of dust left over after lunar impacts the outermost ring is Phoebe.

1.9.5 Saturn's Rings Shine in Hubble's Latest Portrait

Saturn is so beautiful that astronomers cannot resist using the Hubble Space Telescope to take yearly snapshots of the ringed world when it is at its closest distance to Earth.

Figure 1.6 : Saturn rings shining [6]

Dynamic Atmosphere:

Saturn's atmosphere is tumultuous and constantly shifting, according to Hubble photos. Little storms come and go quickly. There are slight color variations in the banded structure.

Durable Attributes: The hexagonal pattern near the North Pole which Voyager 1 found in 1981 [7]—remains constant.

Value to Science: Superior clarity enables in-depth analysis of Saturn's atmosphere. Annual observations monitor changes and trends in the weather. The OPAL project benefits from Hubble data, which advances our knowledge of the atmospheres of gas giant planets. Saturn's iconic rings

continue to be breathtaking. The ring system is oriented toward Earth, as the photograph shows, offering spectators a breathtaking vista of the dazzling, glittering structure. Many ringlets and the fainter inner rings are resolved by Hubble.

1.10 Physical Effects

1.10.1 Pressure term

On Jupiter and Saturn, pressure is a major factor in the formation and behavior of vortices, or massive storms. This is how the extreme pressure found in the atmospheres of Jupiter and Saturn functions as a constraining force, compressing the gases and assisting the vortices in keeping their distinct forms. If there wasn't enough pressure, the storms would probably blow over. Energy Source: Gas is compressed and heated as it moves toward the center of a vortex as a result of pressure differences. The storm's internal circulation is fueled by this transformation of potential energy (because of position) into thermal energy (heat).

Pressure Variations within a Vortex:

Pressure increases as altitude decreases. In the vortex, vertical circulation arises due to pressure difference. Cooler air sinks to the periphery as warmer air ascends in the core. This circulation maintains the structure and intensity of the storm. Horizontal winds can originate from pressure variations within a vortex. These winds contribute to the storm's rotation and churning.

Impact on Different Types of Vortices:

The atmospheric pressure rises as you go deeper into the atmosphere. The vortex experiences a vertical circulation due to the pressure difference within it. As a result of higher pressure at the periphery, warm air rises in the center and cold air descends. The storm's shape and intensity are sustained by this circulation. Horizontal winds can result from pressure variations within a vortex. The winds contribute to the storm's overall rotation and churning.

Uncertainties and Further Research:

The relationship between pressure and vortex behavior is intricate and unclear. The Coriolis force and interactions with neighboring air waves, in addition to the planet's rotation, affect atmospheric

circulation. Scientific research is ongoing to understand the impact of pressure changes on vortex development, evolution, and strength in Jupiter's and Saturn's deep atmospheres. Pressure significantly contributes to the formation and upkeep of Jupiter and Saturn's powerful vortices. Studying the interaction between atmospheric pressure and storms aids in comprehending the workings of massive planets' atmospheres.

1.10.2 Viscosity term

The influence of a fluid's viscosity on vortex dynamics, such as Jupiter's Great Red Spot, is significant. Below is a discussion of how viscosity impacts the formation and behavior of massive atmospheric vortices.

Energy Dissipation: A fluid's viscosity determines its resistance to deformation. In Jupiter and Saturn's atmospheres, viscosity causes energy loss within vortices. With increasing viscosity, energy loss escalates, leading to weaker vortices. Due to Jupiter's low viscosity atmosphere and slow energy dissipation, the Great Red Spot has lasted for centuries.

Vortex Structure: Vortices' stability and structure depend on viscosity. In stable, low-viscosity atmospheres, vortices form with clear-cut boundaries. A higher viscosity may lead to less distinct vortices with indistinct edges. The Great Red Spot on Jupiter retains its unique and persistent form due to the planet's low atmospheric viscosity.

Interaction with Surrounding Flows: Vortices' interaction with airflows is influenced by viscosity. In low viscosity conditions, vortices can absorb smaller eddies or merge with others more efficiently, leading to more complex interactions. In highly viscous environments, these interactions can cause vortices to lose coherence or dissipate more rapidly.

Heat and Momentum Transfer: Viscosity affects the transfer of heat and momentum within and outside a vortex. On Jupiter and Saturn, where viscosity is low, turbulent processes dominate for heat and momentum transmission rather than viscous diffusion. The durability and dynamic nature of vortices are enhanced by this.

Scale and Lifetime: The size and lifespan of vortices are influenced by viscosity. At lower viscosities, larger and more persistent vortices may form. The Great Red Spot's longevity in

Jupiter's low-viscosity atmosphere is over 400 years. The vortex's form and energy are preserved through extended periods thanks to this.

The great Red Spot and Saturn's hexagonal storm persist due to the low viscosity of their atmospheres. Due to the slow energy release and complex engagements with nearby air currents, these vortices remain stable for extended durations.

1.10.3 Corlious force term

The atmospheric vortices on Jupiter and Saturn are significantly affected by the Coriolis force. The Coriolis force influences these large atmospheric vortices.

Vortex Formation and Rotation: The Coriolis force, arising from the planet's rotation, acts perpendicularly to the air particles' motion. This force causes the development and spinning of massive vortices on Jupiter and Saturn by disrupting their air circulation. On planets with a Coriolis force, moving air is deflected to the left in the southern hemisphere and to the right in the northern. The northern hemisphere counter-rotates from the southern hemisphere.

Vortex Stability and Maintenance: The Coriolis force stabilizes vortices by counterbalancing the pressure gradient force. In a vortex, the Coriolis force counteracts the pressure gradient force, which is directed from high to low pressure. The equilibrium maintains the vortex's coherence and prevents its premature dissipation.

Size and Scale of Vortices: The Coriolis force exhibits maximum strength at the poles and minimum strength at the equator. Its strength varies with latitude and intensifies with the planet's faster rotation rate. Rapidly rotating planets like Jupiter and Saturn are capable of forming large-scale vortices due to a strong Coriolis Effect. The Coriolis force and pressure gradients maintain the existence of the Great Red Spot, an immense anticyclone storm on Jupiter.

Meridional Circulation and Vortex Drift: The Coriolis force influences both the meridional circulation and vortex drift in the atmosphere. The vortex's direction could change latitudinal due to the influences of surrounding forces. This drift alters the dynamics of the planet's atmosphere, leading to the redistribution of momentum and heat. The Coriolis force influences both the meridional circulation and vortex drift in the atmosphere.

Interaction with Zonal Jets: Jupiter and Saturn are distinguished by their strong zonal jets, which are east-west winds. The Coriolis force affects these jets as well. These jets can modify vortices' sizes, shapes, and trajectories through their interactions. The Coriolis force maintains the stability of zonal jets, influencing air vortex behavior.

The Coriolis force significantly influences the formation, rotation, stability, and behavior of vortices on Jupiter and Saturn. It facilitates the growth of major storms, manages their interaction with other atmospheric occurrences, and maintains their structural integrity through pressure equilibrium.

1.10.4 Electric potential term

In the presence of fluid mechanics and planetary rotation, the electric potential's influence on atmospheric vortices like Jupiter's and Saturn's is less pronounced compared to the effects of viscosity and the Coriolis force. Electric forces can also influence gas giants' atmospheres.

Electrostatic Forces on Particles: The complex magnetospheres of Jupiter and Saturn generate potent electric fields. These fields can influence the charged particles in the atmosphere. Electrostatic forces can influence the distribution and movement of charged dust and ice particles within vortices. Modifying the storm could alter its cloud and lightning patterns.

Lightning and Electric Discharges: The vortices on Jupiter and Saturn exhibit lively lightning activity [7]. Lightning strikes create electric fields in the atmosphere from convective storms. Producing pressure waves and heating the surrounding gases could affect vortices' dynamics and structure.

Magnetosphere Interactions: The magnetic field of the planet induces electric currents in the atmosphere. Down its magnetic field lines, strong currents flow from Jupiter into Io's atmosphere. These currents can trigger auroras and possibly influence atmospheric circulation patterns, thereby affecting vortices.

Charged Particle Dynamics: In ionized atmospheres, such as those above thunderstorms, magnetic and electric fields can influence charged particles. Ionization can affect the local

electrical environment and potentially influence small-scale vortex dynamics and air particle behavior.

Potential Effects on Cloud Chemistry: Electric fields can influence the chemical reactions happening in Jupiter's and Saturn's clouds. These molecules and complex hydrocarbons in the atmosphere could potentially be influenced by their synthesis. Cloud chemical composition alterations influence both buoyancy and radiative properties, impacting vortex behavior.

Though electric forces and fields can have secondary impacts, the primary influences on the dynamics of vortices on Jupiter and Saturn are fluid mechanics and planetary rotation. These activities encompass interacting with magnetosphere currents, modifying cloud chemistry, shaping charged particle dynamics, and instigating electric discharges and lightning. While less extensive and particular, these effects can significantly alter the behavior of atmospheric vortices on gas giants.

1.10.5 Drag forces terms

Compared to the forces (pressure, viscosity) previously stated, the drag force resulting from the relative speed of dust particles and charged and neutral particles in Jupiter's and Saturn's vortices is probably negligible. This is an explanation:

Dust Particles:

Low Concentration: Compared to the two main atmospheric gases (helium and hydrogen), dust particles are found in significantly lower amounts. This indicates that their total effect on the dynamics of the vortex is smaller. Dust particles possess a higher inertia and are comparatively larger in size when compared to gas molecules. They are therefore less vulnerable to the faster-moving gas's drag forces.

Drag forces significantly influence the dynamics of Jupiter and Saturn's atmospheric vortices by dissipating energy, shaping vortexes, and interacting with atmospheric layers and zonal jets. Despite their long endurance, big vortices' behaviors are persistently altered by varying drag forces.

1.11 Problem Statement

The formation, evolution, and mutual interactions between the atmospheric vortices in Jupiter and Saturn are studied. The dynamics and stability of these systems are regulated by their physical mechanisms. The internal energy processes of these planets impact how they behave. The gas giants Jupiter and Saturn boast stunning atmospheric vortices as captivating features. Dynamic structures significantly impact the planets' weather and atmospheric circulation. Despite elaborate studies, the intricate dance of these vortices remains a mystery. The study intends to illuminate the significant aspects mentioned below.

Formation and Evolution:

The birth of these vortices is triggered by certain physical mechanisms. Do interactions with the planets' rotation and existing wind patterns play a more significant role in atmospheric churning than deep-seated convection? The time evolution of these vortices is described in the text. They may either intensify or weaken. Do they either merge or dissipate? Knowing their life cycle is essential to fully grasp their overall influence on the atmosphere.

Interaction Dynamics:

How do neighboring vortices interact with each other? Do they repel, attract, or merge, creating even larger storm systems? How do these interactions influence the surrounding atmospheric flow? Do they create zones of turbulence or channel winds in specific directions?

Governing Mechanisms:

What physical principles govern the stability and dynamics of these vortices? Is it a balance between pressure forces, Coriolis effects (due to planetary rotation), and internal friction (viscosity) within the gas giants' atmospheres? How do the strong winds, known as zonal jets, surrounding these vortices influence their behavior?

Internal Energy Processes: How do the internal heat sources of Jupiter and Saturn, possibly originating from their cores, influence the formation and evolution of these vortices? Does this internal heat play a role in powering the atmospheric dynamics or act as a stabilizing force?

Expanding the Scope:

Through a comparison of Jupiter's and Saturn's vortex behaviors, we can determine whether there are universal principles or unique factors influencing these phenomena.

Ultimately, unraveling these mysteries will lead to:

Understanding the complex atmospheric behaviors of Jupiter and Saturn in depth. Advanced climate models for gas giants yield more accurate forecasts of their future atmospheric conditions. Examining the development and transformation of atmospheres on exoplanet twins. To unravel the secrets hidden within the swirling storms of Jupiter and Saturn, we will need to utilize data from space missions such as Juno and Cassini, coupled with advanced computer simulations and theoretical modeling.

Based on data from the WFC3/UVIS instrument on board the Hubble Space Telescope (HST), we presented a theory describing the effect of zonal jets in the Great Red Spot (GRS) of Jupiter. The charged dust cloud and neutrals with background of un-bounded plasma is used as a modelling tool for driven-dissipative complex flow systems in nature. We predicted structural variations of self-organized vortices in Jupiter's atmosphere, such as the GRS and White Ovals. The steady state flow linear and nonlinear solutions are obtained using a 2D hydrodynamic model. The atmosphere of Jupiter, the largest planet in the solar system, supports a variety of dynamical behavior, ranging from micro-level turbulence and instabilities to macro-scale stable zonal jets and vibrant vortices (Marcus, 1993; Marcus, 1993; Vasavada et al., 1998). The Great Red Spot (GRS), White Ovals, as well as band structured Belts and Zones connected with the sheared zonal jets are the most prominent aspects in atmosphere of Jupiter. Several fluid models that include the concept of potential vorticity deduce vortices as Rossby solitons. The flow profiles, ongoing structural variations and horizontal drift velocity are only a few of the many critiques that have been levelled with this concept (Marcus and Lee, 1994; Dowling and Ingersoll, 1989). Additionally, it has been suggested that the energy from small-scale eddies and moist convection from the deep interior of Jupiter's interior drive both the streaming zonal jets and the vortices of its atmosphere (Ingersoll et al., 2000). However, it is unlikely that these processes are the primary causes of such massive vortices.

1.12 Motivation

Space phenomena on gas giants like Jupiter and Saturn greatly differ from those on Earth. These planets possess intriguing long-lasting vortices, like Jupiter's Great Red Spot and Saturn's polar hexagon. The origin and energy source of these large atmospheric structures, which have endured for centuries, continue to elude scientists.

Understanding Long-Lasting Vortices

Hurricanes and tornadoes on Earth usually dissipate within days to weeks due to interactions with land and atmospheric conditions. On gas giants, vortices persist for much longer durations, implying distinct energy retention and stability mechanisms. Decoding these mechanisms poses a significant scientific hurdle. Discovering the causes of these alien vortices' longevity could shed light on fluid dynamics under extremely dissimilar circumstances.

Potential for Energy Storage

These long-lasting vortices harbor immense energy. On Earth, we are persistently exploring methods for enhancing energy storage and management. Analyzing Jupiter's GRS or Saturn's hexagon energy patterns could potentially lead to advancements in terrestrial energy storage systems. Understanding the energy maintenance of vortices could introduce innovative energy storage methods, drastically changing energy management and sustainability.

Mitigating Natural Disasters

Understanding the stability of vortices on gas giants could enhance Earth's ability to predict and lessen the impact of short-term vortices. Severe weather phenomena such as hurricanes, typhoons, and tornadoes pose major risks to both life and property. Understanding energy dynamics and stability of extraterrestrial vortices can potentially lead to innovative ways to predict and manage these destructive weather occurrences, thereby improving our capacity to safeguard communities and mitigate financial damages. Understanding the stability of vortices on gas giants could enhance Earth's ability to predict and lessen the impact of short-term vortices. Severe weather phenomena such as hurricanes, typhoons, and tornadoes pose major risks to both life and property. Understanding the stability of vortices on gas giants could enhance Earth's features.

Advancing Scientific Knowledge

Studying long-lasting vortices on gas giants not only provides practical insights but also enhances our knowledge of planetary atmospheres and fluid dynamics. These insights can significantly expand our understanding of planetary formation and evolution, as well as enhance our models of atmospheric behavior on Earth and throughout the solar system.

The motivation for studying long-lasting vortices on gas giants is multifaceted. This field covers scientific exploration, advanced energy storage innovations, and effective disaster prevention tactics. Unraveling the secrets of these atmospheric phenomena opens doors to novel discoveries in planetary science and practical applications for life on Earth.

As we know that the Jupiter and Saturn atmosphere is mainly composed of hydrogen and helium gases. And we also know that these two light gases are also must abundant on sun. so by studying these giants planets we can also predict the dynamics of sun in a better way. Also we can these two planets are far away from sun so there might be a possibility that these planets dynamics can give us idea about formation of universe. The motivation for studying long-lasting vortices on gas giants is multifaceted. This field covers scientific exploration, advanced energy storage innovations, and effective disaster prevention tactics. Unraveling the secrets of these atmospheric phenomena opens doors to novel discoveries in planetary science and practical applications for life on Earth. Understanding the stability of vortices on gas giants could enhance Earth's ability to predict and lessen the impact of short-term vortices. Severe weather phenomena such as hurricanes, typhoons, and tornadoes pose major risks to both life and property. Understanding energy dynamics and stability of extraterrestrial vortices can potentially lead to innovative ways to predict and manage these destructive weather occurrences, thereby improving our capacity to safeguard communities and mitigate financial damages. Understanding the stability of vortices on gas giants could enhance Earth's ability to predict and lessen the impact of short-term vortices. Severe weather phenomena such as hurricanes, typhoons, and tornadoes pose major risks to both life and property. Understanding the stability of vortices on gas giants could enhance Earth's features. Space phenomena on gas giants like Jupiter and Saturn greatly differ from those happening on Earth. These long-lasting vortices harbor immense energy. On Earth, we are persistently exploring methods for enhancing energy storage and management.

1.13 Objectives

1.13.1 Developing a Theoretical Model for the Dynamics of Long-Lasting Vortices in Gaseous Giants

To develop a comprehensive theoretical framework explaining the formation, evolution, and stability of lengthy-lasting atmospheric vortices on gas giants such as Jupiter and Saturn. Investigate the initial conditions that lead to vortex formation, such as atmospheric pressure gradients, differential heating, and turbulence. Analyze the development, maturity, and interactions of atmospheric vortices in the context of long-term evolution. Analysis encompasses the effects of planetary rotation, heat transfer, and fluid dynamics. Determine the underlying physical causes that ensure vortices' enduring existence. Consider the equilibrium of pressures, Coriolis Effect, and atmospheric composition and structure. Develop and test computational models simulating vortex behavior under varying conditions. Gain analytical insights into vortex dynamics via these models.

1.13.2 Comparing the Vortices of Gaseous Giants with Solid Planets

Compare and contrast the atmospheric vortices' characteristics, dynamics, and stability on gaseous giants versus those on solid planets like Earth and Mars. On gaseous giants, the absence of a solid surface affects vortex formation and stability differently than on solid planets due to the lack of topography and surface interactions. Comparing the atmospheric compositions, pressure profiles, and temperature gradients of gaseous giants and solid planets is crucial for understanding the resulting vortex behavior. Investigate the impact of varying rotation rates and planetary sizes on the Coriolis force, and how it alters vortex dynamics for gaseous giants in contrast to solid planets. Analyzing the dynamics and stability of vortices, like Jupiter's Great Red Spot, Saturn's polar hexagon, and Earth's cyclones and anticyclones, involves examining their unique characteristics.

1.13.3 Studying the Reasons behind Stable Vortices

To explore the causes behind the prolonged stability and persistence of certain atmospheric vortices, specifically on gaseous giants. Investigate the role of internal heat sources, solar radiation, atmospheric convection, and energy dissipation mechanisms in maintaining the energy equilibrium of vortices. Analyze the interactions between vortices and the prevailing east-west

winds (zonal jets) on gaseous giants. Grasp the role these interactions play in preserving and sustaining vortices. Investigate the impact of planetary magnetic fields and electric forces on vortex stability. Evaluate how charged particle dynamics and lightning affect various systems. Vortices' stability is affected by celestial impacts and gravitational interactions with moons.

1.13.4 Research Approach

Devise mathematical models and theoretical frameworks for explaining vortices' formation, evolution, and stability. Apply fluid dynamics, thermodynamics, and planetary science principles to analyze complex natural phenomena. Conduct high-resolution numerical simulations to model vortex dynamics under diverse atmospheric conditions. Validate the models using data obtained from space missions and telescopes. Conduct comparative analyses of gaseous giants and solid planets using observational data, simulations, and theoretical models. Combine observational data from space missions like Voyager, Galileo, Cassini, and Juno, ground-based telescopes, and atmospheric probes to validate and inform theoretical models and simulations. Perform controlled laboratory experiments to investigate vortex dynamics in environments analogous to the atmospheres of gaseous giants and solid planets.

1.13.5 Expected Outcomes

A theoretical model that comprehensively explains the longevity and stability of vortices on gaseous giants. Insights into the distinctions and overlaps of vortices on gaseous giants and solid planets are meticulously explored. Advanced knowledge of atmospheric vortex stability, applicable to planetary science and fluid dynamics. Improved understanding of vortex behavior enhances observational data interpretation and future mission planning.

Conduct comparative analyses of gaseous giants and solid planets using observational data, simulations, and theoretical models. Combine observational data from space missions like Voyager, Galileo, Cassini, and Juno, ground-based telescopes, and atmospheric probes to validate and inform theoretical models and simulations. Perform controlled laboratory experiments to investigate vortex dynamics in environments analogous to the atmospheres of gaseous giants and solid planets. To explore the causes behind the prolonged stability and persistence of certain atmospheric vortices, specifically on gaseous giants. Investigate the role of internal heat sources.

1.14 Scope of the thesis

1.14.1 Coverage

The intricate origins of vortices in Jupiter and Saturn's atmospheres through comprehensive research. The interplay between differential heating, pressure gradients, and atmospheric turbulence drives vortex generation.

This study examines the mechanisms driving the expansion, progression, and dissipation of atmospheric vortices. This study examines the impact of planetary rotation, heat transfer, and fluid dynamics on vortex development. Studying the relationships between vortices and atmospheric structures such as zonal jets and other vortices. Examination of the interactions between vortices and surrounding atmospheric features, including zonal jets and other vortices.

Examining the underlying physical processes enabling the sustained existence and persistence of atmospheric vortices. The impact of viscosity, Coriolis force, drag forces, and electric fields on vortex stability must be considered. The stability of vortices in planets is upheld by internal energy processes, including heat fluxes from their interiors. Investigation of the role of internal energy processes, such as heat fluxes from planetary interiors, in maintaining vortex stability.

This study compares the characteristics, dynamics, and stability of atmospheric vortices on gaseous giants, Jupiter and Saturn, and solid planets, including Earth and Mars. Vortex dynamics are impacted by variations in atmospheric composition, pressure profiles, temperature gradients, and surface interactions. Examination of how differences in atmospheric composition, pressure profiles, temperature gradients, and surface interactions influence vortex dynamics.

We develop high-resolution numerical simulations to model vortex dynamics under various atmospheric conditions using theoretical and computational methods. Through fluid dynamics theories, analytical models and insights into vortex behavior are derived. Through the combination of observational data from both space missions and ground-based telescopes, theoretical models and simulations can be validated.

1.14.2 Exclusions

The study will focus on atmospheric composition's effect on vortex dynamics but won't examine the intricacies of chemical reactions and microphysical processes occurring within the vortices.

The study will concentrate on the vortices found on gaseous giants and certain solid planets (Earth and Mars). On non-gaseous planets and moons, vortices will not be discussed extensively. Vortices on other non-gaseous planets or moons will not be extensively covered.

Instead of exploring transient or localized phenomena such as small-scale storms and short-lived atmospheric disturbances, the thesis will concentrate on large-scale, long-lasting vortices. The thesis will focus on large-scale, long-lasting vortices rather than transient or localized weather phenomena such as small-scale storms or short-lived atmospheric disturbances.

The impact of electric fields and lightning activity on vortex dynamics will not be the focus of this study concerning magnetosphere and ionosphere interactions. Magnetosphere and Ionosphere Interactions: Although the influence of electric fields and lightning activity on vortex dynamics will be considered, detailed studies on magnetosphere and ionosphere interactions will be outside the scope of this research.

The study will largely depend on theoretical modeling, numerical simulations, and observational data in the laboratory setting. This study will prioritize field research over laboratory experiments. While laboratory experiments might provide supplementary insights, they will not be a primary focus of this study.

Although applicable fluid dynamics principles will be examined, this study will primarily focus on atmospheric vortices on Earth's oceans. Vortices on Earth’s Oceans: The study will focus on atmospheric vortices rather than oceanic vortices, although fluid dynamics principles applicable to both will be explored. This research aims to give a focused, in-depth, and comprehensive understanding of vortex dynamics on Jupiter and Saturn.

1.15 Thesis Layout

This thesis includes five chapters. **Chapter 1** consists of introduction. **Chapter 2** provides information about literature review. Methodology is discussed in **Chapter 3**. Results are provided in **Chapter 4**. The thesis is concluded in **Chapter 5**.

Chapter 2: Literature Survey

The atmosphere of Jupiter, the largest planet in the solar system, supports a variety of dynamical behavior, ranging from micro-level turbulence and instabilities to macro-scale stable zonal jets and vibrant vortices (Marcus, 1993 [8]; Vasavada et al., 1998 [9]). The Great Red Spot (GRS), White Ovals, as well as band structured Belts and Zones connected with the sheared zonal jets are the most prominent aspects in atmosphere of Jupiter (Simon et al., 2014 [10]; Choi, et al., 2010 [11]; Marcus and Shetty, 2011 [12]). At central latitude 22.3^0 S of Jupiter (where 1° = 1160 km), the GRS is an incredible, enduring large anticyclone cloud vortex with dimensions of 14.1° longitude and 9.4° latitude (Simon et al., 2018 [13]), while the White Ovals are comparatively small vortices seen at latitudes 33.8° S, 41.8° S, and 19.0° N (Vasavada et al., 1998 [9]; Choi et al., 2010 [11]; Marcus and Shetty, 2011 [12]). White Ovals and GRS both have dormant central regions of symmetric vorticity surrounding by collar rings of fast flow that separate the central regions from adjacent feeble flows (Vasavada et al., 1998 [9]; Mitchell, et al., 1981 [14]).

The previously observed characteristics in atmosphere of Jupiter have been confirmed by NASA's spacecraft (Juno-2018) including the interior rotating period of GRS is decreasing, the giant vortex is contracting at a rate of 0.19°/year along latitude and 0.048°/year along longitude. The inclusive shape is becoming more circular with passage of time and barely noticeable changes in the flowing zonal jets are seen (Simon et al., 2014 [10]; Simon, et al., 2018 [13]). Many mysteries adjoining the physical explanation in vortices of Jupiter such as the driving mechanism, drift of GRS on the plane, the continual shape change, the existence of collar rings of fast flow in the dormant core, the long-lasting perseverance of the vortices, and the actual 3D shape, among others are still unrevealed even subsequently several decades of observations and analysis (Vasavada et al., 1998 [9]; Simon et al., 2014 [10]; Rogers, 2008 [15]; Simon-Miller, et al., 2002 [16]). According to Sun et al., 2018 [17] both exciting (turbulence) and trapping (bulk transport) mechanisms are used by terrestrial ocean eddies to convey heat meridionally. Though trapping could be considerable on Saturn, where pole-ward migration of the anticyclone produced by the 2010 Great White Storm (Hueso et al., 2020 [18]; Sayanagi et al., 2013 [19]). Marcus, 2004 [20] anticipated that the exciting mechanism, which is governed by the chaotic behavior of three white ovals close to 34° S at Jupiter, could transform, possibly resulting in a change in temperature at that latitude. But the evidence is questionable given that later Oval changed its color back to white (Simon, 2015 [21]).

Wong et al. 2021 [22] acquired Data by HST/WFC3 (Dressel, 2021 [23]) over the time period 2009–2020 and used the Advection Corrected Correlation Image Velocimetry (ACCIV) method to recover the velocity field. This method was created specifically to measure velocities along curved routes in Jupiter's anticyclones (Asay-Davis et al., 2009 [24]; Asay-Davis, 2015) [25]. Several fluid models that include the concept of potential vorticity deduce vortices as Rossby solitons. The flow profiles, ongoing structural variations and horizontal drift velocity are only a few of the many critiques that have been levelled with this concept (Marcus and Lee, 1994 [26]; Dowling and Ingersoll, 1989 [27]). Additionally, it has been suggested that the energy from small-scale eddies and moist convection from the deep interior of Jupiter's interior drive both the streaming zonal jets and the vortices of its atmosphere (Ingersoll et al., 2000 [28]). The GRS and White Ovals, on the other hand, are described as complex flow systems made up of a variety of species, including NH_3, CH_4, Ar, NH_4SH, H_2O-ice, dust and charged particles that are in dynamic equilibrium with the zonal jets and other forcing factors like the Coriolis force and thermo-convection moist (Marcus, 1993 [8]; Loeffler et al., 2016 [29]; Weidenschilling and Lewis, 1973 [30]). Moreover, the position and shear intensity of the streaming jets, which think to be the primary source of the vortices on Jupiter are significantly connected with the size, strength, and direction of the vortices in the planet's banded structure (Vasavada et al., 1998 [9]; Choi, et al., 2010 [11]; Mitchell, et al., 1981 [14]; Rogers, 2008 [15]). It has been demonstrated that GRS has extensive relatively stable vertically divided deeper layers inside of thin, wide upper layers, which have minimal effect on the dynamics of the uppermost layers (Marcus, 1993 [8]; Vasavada et al., 1998 [9]).

The major goal of this study is to give the theory that describes the dynamical characteristics of the GRS, which is based on data (Wong et al. 2021 [22]) from the WFC3/UVIS instrument on board the Hubble Space Telescope (HST). In reality, higher dimensional nonlinear partial differential equations (NPDEs) should be used to represent the linear and nonlinear dynamics of the real planetary atmosphere. The KdV equation and the mKdV equation in (2 + 1) dimensional situations have been examined by several researchers in a variety of scientific fields, including plasma physics, space science, ion-acoustic waves, shallow water waves, and others (Kadomtsev and Petviashvili, 1970 [31]; Groves and Sun, 2008 [32]; Infeld and Rowlands, 2001 [33]; Zakharov and Kuznetsov, 1974 [34]). It is commonly known that the (2 + 1) dimensional model equations of Kadomtsev-Petviashvili and Zakharov-Kuznetsov are used to describe shocks, solitons and

vortex dynamics (Kadomtsev and Petviashvili, 1970 [31]; Zakharov and Kuznetsov, 1974 [34]). These models effectively explain the underlying physical phenomena. Guinn and Schubert 1993 [35] study was a significant step forward in the understanding of hurricane spiral bands. The movement of the fluid can be seen approximately on xy (2-dimensional) motion on the plane (See Wong et. al., 2021 [22]).

The modified Naiver stokes equation can be used accurately account for both the drive given by ion drag and the friction caused by stationary neutral fluids (Landau and Lifshits, 1987). The mean absolute value of the relativity vorticity and her parameters, L_x zonal length scale, L_y meridional length scale, H atmospheric height, g gravity of Jupiter, L_o zonal characteristics length are obtained from the article data based on WFC3/UVIS instrument on board the HST (Dressel, 2021 [23]). Length and velocity-scales correspond to the radius of maximum winds (RMW) and the maximum tangential velocity and U_0 is the characteristic zonal velocity scale inserted from the available onboard data (Wong et al., 2021 [22]). The variation in frequency obtained at three different values of kinematic viscosity corresponding to Jupiter atmosphere at $10^7 m^2/sec$,$2 \times 10^7 m^2/sec$, and $5 \times 10^7 m^2/sec$ (Vidmachenko, 1986 [36]) We observed that the GRS's Rossby number did not correspond to long-term patterns. Because shear in the environment of vortices produces deviations from circular shape (e.g., Marcus, 1990 [37]; Moore & Saffman, 1971 [38]), a decrease in the amount of the anticyclonic shear in the surrounding flow could explain a long-term change in aspect ratio. We presented the mathematical model to describe the structure, stability and shape of the vortex dynamics. Whereas, vortex models confined by imaging and wind field data have been widely employed to predict atmospheric static stability on Jupiter (Brueshaber & Sayanagi, 2021 [39]; Brueshaber et al., 2019 [40]; Cho et al., 2001 [41]; Shetty & Marcus, 2010 [42]). One noteworthy drawback of this model is its 2D representation, although real 3D effects from the interior could be anticipated (Ingersoll et al., 2000 [28]).

Chapter 3: Methods Developed

3.1 Magneto hydrodynamics (MHD)

Electrically conducting fluids are the subject of study in the realm of magneto hydrodynamics (MHD). Among these, the models treating plasma as an ideal hydro magnetic fluid are the most efficacious at explaining the equilibrium and wide-scale stability properties of magnetized plasmas. The resistive MHD models have been adopted to study tearing modes and magnetic reconnection in which plasma has finite resistivity that is likely to alter the topology of the magnetic field and the co.

So whenever we have a situation where magnetic effects are prominent than other factors than we can use MHD. If we look on our problem, Jupiter have magnetic field around 417.0 μT and Jupiter have magnetic field around 21 μT. So due to minor effects of magnetic field we are not going to use this model.

If the magnetic field on Jupiter and Saturn is weak and does not play a significant role in the dynamics of atmospheric vortices, we can focus on a purely hydrodynamic model. This approach simplifies the problem to studying the fluid dynamics governed primarily by the Naiver-Stokes equations.

3.2 A Two-Fluid Model

A two-fluid model is a framework used to describe the behavior of two distinct, interacting fluids within a system. This model is particularly useful in a variety of physical contexts, including plasma physics, super fluidity, and astrophysics. In two distinct fluids, fluid 1 can be an electron fluid in plasma, a superfluid component in superfluid helium, or any other type of fluid depending on the context. Fluid 2 can be an ion fluid in plasma, a normal fluid component in superfluid helium, or another distinct fluid.

3.3 Naiver-Stokes Equation

It is the fundamental equation to find any kind of fluid motion equation. The Naiver-Stokes equation can be derived from some conservations and continuity equation when combined with fluids properties. To derive the fluid equation we need to understand the continuity equation and

how it describes the condition for conservation, then we need to introduce the conservations of mass and momentum to find the desired fluid equation.

3.3.1 Continuity equation

A continuity equation or transport equation is an equation that describes the transport of some quantity. It is particularly simple and powerful when applied to a conserved quantity, but it can be generalized to apply to any extensive quantity. Since mass, energy, momentum, electric charge and other natural quantities are conserved under their respective appropriate conditions, a variety of physical phenomena may be described using continuity equations. The continuity equation is a specific mathematical expression of the principle of conservation of mass in fluid dynamics. They are closely related, with the continuity equation providing a local form of mass conservation. Let's derive the continuity equation from the conservation of mass principle.

3.3.2 Conservation of mass principle.

According to the conservation of mass principle, the total mass of a closed system must never change.

Both the net flux of mass across the control volume's boundary and the rate of mass change within it must be zero.

$$\frac{d}{dt}\int_v \rho dV + \int_{\partial V}(\rho \boldsymbol{u}).\boldsymbol{n}dA = 0 \tag{3.1}$$

We apply the Reynolds Transport Theorem to manage the time derivative of an integral over a moving control volume:

$$\frac{d}{dt}\int_v \rho dV = \int_v \frac{\partial \rho}{\partial t} dV + \int_{\partial V}(\rho \boldsymbol{u}).\boldsymbol{n}dA \tag{3.2}$$

Integrate the Reynolds Transport Theorem into the mass conservation integral form:

$$\int_v \frac{\partial \rho}{\partial t} dV + \int_{\partial V}(\rho \boldsymbol{u}).\boldsymbol{n}dA + \int_{\partial V}(\rho \boldsymbol{u}).\boldsymbol{n}dA = 0 \tag{3.3}$$

To change the surface integral into a volume integral, use the Divergence Theorem:

$$\int_{\partial V} \rho \boldsymbol{u}.\boldsymbol{n} dA = \int_{v} \boldsymbol{\nabla}.(\rho \boldsymbol{u}) dV \tag{3.4}$$

Simplifying: Now, the equation becomes:

$$\int_{v} \left(\frac{\partial \rho}{\partial t} \boldsymbol{\nabla}.(\rho \boldsymbol{u}) \right) dV = 0 \tag{3.5}$$

The integrand needs to be zero throughout the control volume V because it is an arbitrary volume. Consequently, the local form of the continuity equation is as follows:

$$\frac{\partial \rho}{\partial t} + \boldsymbol{\nabla}.(\rho \boldsymbol{u}) = 0 \tag{3.6}$$

The idea of conservation of mass is expressed mathematically in the continuity equation. It guarantees that mass is conserved in a fluid flow by stating that the rate of change of fluid density at any point plus the divergence of the mass flux at that point equals zero.

The density of an incompressible fluid is constant. The simplest form of the equation is obtained by dividing by a constant ρ while maintaining the derivative of density at zero.

$$\boldsymbol{\nabla}.\boldsymbol{u} = 0 \tag{3.7}$$

3.3.3 Conservation of momentum

Using Newton second law,

$$\Sigma \boldsymbol{F} = m\boldsymbol{a} \tag{3.8}$$

Put **F** = **b** (body forces) and substitute density for mass we get,

$$\boldsymbol{b} = \rho \frac{d}{dt} \boldsymbol{u}(x, y, z, t) \tag{3.9}$$

Applying chain rule to derivative of velocity

$$\boldsymbol{b} = \rho\left(\frac{\partial \boldsymbol{u}}{\partial t} + \frac{\partial u}{\partial x}\frac{\partial x}{\partial t} + \frac{\partial u}{\partial y}\frac{\partial y}{\partial t} + \frac{\partial u}{\partial z}\frac{\partial z}{\partial t}\right) \tag{3.10}$$

Or

$$\boldsymbol{b} = \rho\left(\frac{\partial \boldsymbol{u}}{\partial t} + (\boldsymbol{u}.\boldsymbol{\nabla})\boldsymbol{u}\right) \tag{3.11}$$

Writing term in parenthesis as $\frac{\boldsymbol{Du}}{Dt}$ we get,

$$\rho\left(\frac{D\boldsymbol{u}}{Dt}\right) = b \tag{3.12}$$

3.3.4 Equations of Motion

The conservation equation lead to the equation of motion for fluids, we assume that the body force on fluid parcels is due to two components, fluid stresses and external forces.

$$b = \boldsymbol{\nabla}.\boldsymbol{\sigma} + f \tag{3.13}$$

Here, σ is the stress tensor and f represents external forces and equation of motion depends on this stress tensor,

Which in equation form is written as,

$$\sigma = -\rho I + T \tag{3.14}$$

Now substitute this in body force equation we get,

$$\rho\frac{D\boldsymbol{u}}{Dt} = -\boldsymbol{\nabla}\rho + \boldsymbol{\nabla}.\boldsymbol{T} + \boldsymbol{f} \tag{3.15}$$

Or

$$\rho\frac{D\boldsymbol{u}}{Dt} = -\boldsymbol{\nabla}\rho + \mu\nabla^2\boldsymbol{u} + \boldsymbol{f} \tag{3.16}$$

Which is most general form of Naiver-Stokes equation.

3.3.5 Viscosity force term

For Newtonian fluid

Shear stress is directly proportional to shear strain rate so,

$$\tau \propto \dot{\varepsilon} \tag{3.17}$$

$$\tau = \mu\dot{\varepsilon} \tag{3.18}$$

Also

$$\text{Shear strain} = \frac{\Delta y}{\Delta x} \text{ or } \frac{\Delta x}{\Delta y} \tag{3.19}$$

$$\tau = \frac{F}{A} \tag{3.20}$$

So

$$F = \tau A \tag{3.21}$$

$$F = \frac{\tau V}{L} \tag{3.22}$$

$$F = \frac{d\tau}{dx} dV \tag{3.23}$$

$$\boldsymbol{F} = \boldsymbol{\nabla}\tau dV \tag{3.24}$$

In x-y plane, we can write

$$\tau = \mu(\dot{\varepsilon_{xy}} + \dot{\varepsilon_{yx}}) \tag{3.25}$$

So

$$\dot{\varepsilon_{xy}} = \frac{\partial}{\partial t}\left(\frac{\Delta y}{\Delta x}\right) \tag{3.26}$$

And

$$\dot{\varepsilon_{yx}} = \frac{\partial}{\partial t}\left(\frac{\Delta x}{\Delta y}\right) \tag{3.27}$$

So

$$\tau = \mu\left(\frac{\partial}{\partial x}V_y + \frac{\partial}{\partial y}V_x\right) \tag{3.28}$$

$$\boldsymbol{\nabla}.\boldsymbol{V} = \frac{\partial V_y}{\partial x} + \frac{\partial V_x}{\partial y} \tag{3.29}$$

Because in shear strain deformation occur perpendicular to the applied force.

So

$$\tau = \mu\boldsymbol{\nabla}.\boldsymbol{u} \tag{3.30}$$

As

$$\boldsymbol{F} = \boldsymbol{\nabla}\tau dV \tag{3.31}$$

So

$$\boldsymbol{F} = \boldsymbol{\nabla}(\mu\boldsymbol{\nabla}.\boldsymbol{u}) \tag{3.32}$$

$$\boldsymbol{F} = \mu\nabla^2\boldsymbol{u}dV \tag{3.33}$$

3.3.6 Pressure gradient force

$$P = \frac{F}{A} \tag{3.34}$$

$$\boldsymbol{F} = PA \tag{3.35}$$

$$\boldsymbol{F} = \frac{PAL}{L} \tag{3.36}$$

$$\boldsymbol{F} = \frac{dP}{dx} dV \tag{3.37}$$

So

$$\boldsymbol{F} = -\boldsymbol{\nabla}\mathrm{P}dV \tag{3.38}$$

3.3.7 Corlious force term

$$\boldsymbol{F} = \boldsymbol{\nabla} PdV \tag{3.39}$$

As

$$P = \frac{dF}{dt} \tag{3.40}$$

$$P = \frac{d}{dt}\left(\frac{mu^2}{r}\right) \tag{3.41}$$

We get

$$P = muw^2 \tag{3.42}$$

As

$$\boldsymbol{F} = \boldsymbol{\nabla}\mathrm{P}dV \tag{3.43}$$

So

$$\boldsymbol{F} = -2\mathrm{wm}\mathbf{u} \tag{3.44}$$

3.3.8 Electric force term

$$\boldsymbol{F} = q\boldsymbol{E} \tag{3.45}$$

And

$$\boldsymbol{E} = -\boldsymbol{\nabla}\phi \tag{3.46}$$

$$\boldsymbol{F} = -\mathrm{q}\boldsymbol{\nabla}\phi \tag{3.47}$$

3.3.9 Drag force term

Drag force due to ion on dust

$$\mathbf{F} \propto (\mathbf{u} - \mathbf{v}) \tag{3.48}$$

u = dust speed

v = ion speed

$$\mathbf{F} = -\chi(\mathbf{u} - \mathbf{v}) \tag{3.49}$$

If u = v then no interaction occurs and force will become zero.

So this force is developed due to difference in relative speed of dust and other particles.

Drag force due to neutral particles on dust

$$\mathbf{F} \propto (\mathbf{u} - \mathbf{w}) \tag{3.50}$$

$$\mathbf{F} = -\eta(\mathbf{u} - \mathbf{w}) \tag{3.51}$$

w = neutral particle speed

Chapter 4: Mathematical Formulation

4.1 Naiver stokes equation:

$$\Sigma \boldsymbol{F} = m\boldsymbol{a} \tag{4.1}$$

$$\boldsymbol{a} = \frac{\Sigma \boldsymbol{F}}{m} \tag{4.2}$$

For total acceleration

$$\boldsymbol{a} = \frac{d\boldsymbol{v}}{dt} \tag{4.3}$$

$$a_{total} = a_{local} + a_{convective} \tag{4.4}$$

Approaches for acceleration:

Lagrangian approach:

It keeps track of individual fluid particles

Here

$$u = u(t) \tag{4.5}$$

It is solved for all particles.

Eulerian approach:

Fixed point in space

$$\boldsymbol{u} = \boldsymbol{u}(x, t) \tag{4.6}$$

For x axis

$$\boldsymbol{u} = \boldsymbol{u}(x, y, z, t) \tag{4.7}$$

$$\boldsymbol{a} = \boldsymbol{a}(x, y, z, t) \tag{4.8}$$

$$\boldsymbol{a_x} = \frac{d\boldsymbol{u}}{dt} \tag{4.9}$$

So

$$\frac{d\boldsymbol{u}}{dt} = \frac{\partial \boldsymbol{u}}{\partial t} + (\boldsymbol{u}.\boldsymbol{\nabla})\boldsymbol{u} \tag{4.10}$$

Here

$$\frac{d\boldsymbol{u}}{dt} = Total\ acceleration \tag{4.11}$$

$$\frac{\partial \boldsymbol{u}}{\partial t} = local\ acceleration \tag{4.12}$$

$$(\boldsymbol{u}.\boldsymbol{\nabla})\boldsymbol{u} = convective\ acceleration \tag{4.13}$$

$$\frac{\partial \boldsymbol{u}}{\partial t} = local\ acceleration \tag{4.14}$$

Here it tells the velocity changes of individual particles

$$(\boldsymbol{u}.\boldsymbol{\nabla})\boldsymbol{u} = Convective\ acceleration \tag{4.15}$$

It is rate of change of velocity with respect to change in position.

It carries information that how surrounding fluid affects the acceleration of individual particle acceleration.

Now

$$\boldsymbol{a} = \frac{\boldsymbol{\Sigma F}}{m} \tag{4.16}$$

$$\frac{d\boldsymbol{u}}{dt} = \frac{\boldsymbol{\Sigma F}}{m} \tag{4.17}$$

$$\frac{d\boldsymbol{u}}{dt} = \frac{1}{m}(\boldsymbol{F}_{pressure} + \boldsymbol{F}_{viscosity} + F_{corlious} + \boldsymbol{F}_{electric\,potential} + \boldsymbol{F}_{drag}) \quad (4.18)$$

Putting values

$$\frac{\partial \boldsymbol{u}}{\partial t} + (\boldsymbol{u}.\boldsymbol{\nabla})\boldsymbol{u} = \frac{1}{m}(-\boldsymbol{\nabla}\mathrm{P}dV + \mu\nabla^2\boldsymbol{u}dV - 2\mathrm{wm}\mathbf{u} + \mathrm{e}\boldsymbol{\nabla}\phi - \chi(\mathbf{u}-\mathbf{v}) - \eta(\mathbf{u}-\mathbf{w})) \quad (4.19)$$

So

$$\frac{\partial \boldsymbol{u}}{\partial t} + (\boldsymbol{u}.\boldsymbol{\nabla})\boldsymbol{u} = \mu\nabla^2\boldsymbol{u} - \frac{\boldsymbol{\nabla}P}{\rho} - 2\Omega u sin\theta\hat{\boldsymbol{r}} + \frac{e}{\rho}\boldsymbol{\nabla}\phi - \chi(\mathbf{u}-\mathbf{v}) - \eta(\mathbf{u}-\mathbf{w}) \quad (4.20)$$

4.1.1 Continuity equation

$$\boldsymbol{\nabla}.\boldsymbol{J} + \frac{\partial \rho}{\partial t} = 0 \quad (4.21)$$

For incompressible fluid with confine volume, we can write

$$\rho \neq \rho(t) \quad (4.22)$$

$$J = \rho u \quad (4.23)$$

$$\boldsymbol{\nabla}.\boldsymbol{J} = 0 \quad (4.24)$$

So

$$\boldsymbol{\nabla}.\boldsymbol{u} = 0 \quad (4.25)$$

Components of velocity

Around z axis in x y direction

$$u(\boldsymbol{x}, \boldsymbol{y}) = U\hat{\boldsymbol{x}} + V\hat{\boldsymbol{y}} \tag{4.26}$$

4.1.2 Stream function

For regular flow

$$E = \boldsymbol{\nabla} V \tag{4.27}$$

If fluid is not rotational then divergence of potential gives field

So for rotational fluid curl of potential gives field

$$\boldsymbol{u} = \boldsymbol{\nabla}\psi \times \boldsymbol{z} \tag{4.28}$$

So

$$U = \frac{\partial \psi}{\partial y} \tag{4.29}$$

And

$$V = -\frac{\partial \psi}{\partial x} \tag{4.30}$$

As

$$\boldsymbol{\nabla}.\boldsymbol{u} = 0 \tag{4.31}$$

So continuity equation is not satisfied

As

$$\frac{\partial U}{\partial x} \neq -\frac{\partial V}{\partial y} \tag{4.32}$$

So using stream function, we can write

$$U = \frac{\partial \psi}{\partial y} \tag{4.33}$$

$$V = -\frac{\partial \psi}{\partial x} \tag{4.34}$$

We get

$$\frac{\partial^2 \psi}{\partial x \partial y} = \frac{\partial^2 \psi}{\partial x \partial y} \tag{4.35}$$

So continuity equation is satisfied.

4.1.3 Beta plane approximation

$$\sin(\alpha + \beta) = sin\alpha cos\beta + cos\alpha sin\beta \tag{4.36}$$

$$\theta = \theta_o + \delta\theta \tag{4.37}$$

$$sin\theta = \sin(\theta_o + \delta\theta) \tag{4.38}$$

So

$$\sin(\theta_o + \delta\theta) = sin\theta_o \cos\delta\theta + cos\theta_o \sin\delta\theta \tag{4.39}$$

For small angle approximation, we can write

$\delta\theta$ is very Small

So $\delta\theta \approx 0$

Or

$$cos\delta\theta = 1 \tag{4.40}$$

As

$$sin\theta = \theta \tag{4.41}$$

And

$$cos\theta = 1 \tag{4.42}$$

$$\sin \delta\theta = \frac{y}{R} \tag{4.43}$$

$$\sin(\theta_o + \delta\theta) = sin\theta_o + cos\theta_o \frac{y}{R} \tag{4.44}$$

$$\sin \theta = sin\theta_o + cos\theta_o \frac{y}{R} \tag{4.45}$$

So

$$2\Omega sin\theta = 2\Omega sin\theta_o + 2\Omega\, cos\theta_o \frac{y}{R} \tag{4.46}$$

Assume vertical component of rotational vector is constant

$$f_o = 2\Omega sin\theta \tag{4.47}$$

$$\beta = \frac{2\Omega\, cos\theta_O}{R} \tag{4.48}$$

It assume f is constant unless y derivative is taken

So

$$2\Omega sin\theta = f_o + \beta(y) \tag{4.49}$$

4.1.4 Linear analysis

Here ignore drag forces as there magnitude is very small

So

$$\frac{\partial \boldsymbol{u}}{\partial t} + (\boldsymbol{u}.\boldsymbol{\nabla})u = \mu\nabla^2\boldsymbol{u} - \frac{\boldsymbol{\nabla}P}{\rho} - 2\boldsymbol{\Omega}\times\boldsymbol{u} + \frac{e}{\rho}\boldsymbol{\nabla}\phi \tag{4.50}$$

Here

$$(\boldsymbol{u}.\boldsymbol{\nabla})\boldsymbol{u} = 0 \tag{4.51}$$

As it is non-linear term

In components

$$\begin{aligned}\frac{\partial}{\partial t}(U\hat{\boldsymbol{x}} + V\hat{\boldsymbol{y}}) = -\frac{1}{\rho}\left(\frac{\partial}{\partial x}\hat{\boldsymbol{x}} + \frac{\partial}{\partial y}\hat{\boldsymbol{y}}\right)P + \mu\left(\frac{\partial^2}{\partial x^2} + \frac{\partial^2}{\partial y^2}\right)(U\hat{\boldsymbol{x}} + V\hat{\boldsymbol{y}}) \\ - 2\left(\Omega\hat{\boldsymbol{z}}\times(U\hat{\boldsymbol{x}} + V\hat{\boldsymbol{y}})\right) + \frac{e}{\rho}\left(\frac{\partial\phi}{\partial x}\hat{\boldsymbol{x}} + \frac{\partial\phi}{\partial y}\hat{\boldsymbol{y}}\right)\end{aligned} \tag{4.52}$$

$$\begin{aligned}\frac{\partial U}{\partial t}\hat{\boldsymbol{x}} + \frac{\partial V}{\partial t}\hat{\boldsymbol{y}} - \frac{1}{\rho}\frac{\partial P}{\partial x}\hat{\boldsymbol{x}} - \frac{1}{\rho}\frac{\partial P}{\partial y}\hat{\boldsymbol{y}} + \mu\frac{\partial^2}{\partial x^2}U\hat{\boldsymbol{x}} + \mu\frac{\partial^2}{\partial y^2}V\hat{\boldsymbol{y}} - 2\Omega U sin\theta\hat{\boldsymbol{y}} \; + 2\Omega V sin\theta\hat{\boldsymbol{x}} \\ + \frac{e}{\rho}\frac{\partial\phi}{\partial x}\hat{\boldsymbol{x}} + \frac{e}{\rho}\frac{\partial\phi}{\partial y}\hat{\boldsymbol{y}}\end{aligned} \tag{4.53}$$

Comparing x and y terms on both sides

We get

$$\frac{\partial U}{\partial t} = -\frac{1}{\rho}\frac{\partial P}{\partial x} + \mu\frac{\partial^2 U}{\partial x^2} + 2\Omega V sin\theta + \frac{e}{\rho}\frac{\partial\phi}{\partial x} \tag{4.54}$$

$$\frac{\partial V}{\partial t} = -\frac{1}{\rho}\frac{\partial P}{\partial y} + \mu\frac{\partial^2 V}{\partial y^2} + 2\Omega U sin\theta + \frac{e}{\rho}\frac{\partial\phi}{\partial y} \tag{4.55}$$

Now after linearizing, we get

$$\frac{\partial U}{\partial t} = -\frac{1}{\rho_o}\frac{\partial P}{\partial x} + \mu\frac{\partial^2 U}{\partial x^2} + 2\Omega V sin\theta + \frac{e}{\rho_o}\frac{\partial\phi}{\partial x} \tag{4.56}$$

$$\frac{\partial V}{\partial t} = -\frac{1}{\rho_o}\frac{\partial P}{\partial y} + \mu\frac{\partial^2 V}{\partial y^2} + 2\Omega U sin\theta + \frac{e}{\rho_o}\frac{\partial \phi}{\partial y} \tag{4.57}$$

Now putting beta plane approximation

$$2\Omega sin\theta = f_o + \beta(y) \tag{4.58}$$

We get

$$\frac{\partial U}{\partial t} - f_o V - \beta V(y) = -\frac{1}{\rho_o}\frac{\partial P}{\partial x} + \mu\frac{\partial^2 U}{\partial x^2} + \frac{e}{\rho_o}\frac{\partial \phi}{\partial x} \tag{4.59}$$

$$\frac{\partial V}{\partial t} + f_o U + \beta U(y) = -\frac{1}{\rho_o}\frac{\partial P}{\partial y} + \mu\frac{\partial^2 V}{\partial y^2} + \frac{e}{\rho_o}\frac{\partial \phi}{\partial y} \tag{4.60}$$

These equations are coupled in U and V, and decoupling them yields independent equations for these variables.

We get

$$\frac{\partial \nabla U}{\partial t} = \mu\frac{\partial^3 U}{\partial x^3} - \frac{1}{\rho_o}\frac{\partial^2 P}{\partial x^2} + \frac{e}{\rho_o}\frac{\partial^2 \phi}{\partial x^2} \tag{4.61}$$

$$\frac{\partial \nabla V}{\partial t} = \mu\frac{\partial^3 V}{\partial y^3} - \frac{1}{\rho_o}\frac{\partial^2 P}{\partial y^2} + \frac{e}{\rho_o}\frac{\partial^2 \phi}{\partial y^2} \tag{4.62}$$

Now we have to write the electric potential in term of velocity

For that purpose

The dust grain initially gets negatively charged because the ion current to it is substantially less than the electron current. This causes the electron and ion currents to fluctuate until electron current and ion current are equalized. [43]

$$j_e = j_i \tag{4.63}$$

$$j_e = n_e e\sqrt{\frac{kT}{m_e}}\left(e^{\frac{e\phi}{kT}}\right) \tag{4.64}$$

$$j_i = n_i e\sqrt{\frac{kT}{M}}\left(1 - \frac{e\phi}{kT}\right) \tag{4.65}$$

Is caused by orbital motion effects $1 - \frac{e\phi}{kT}$

As we know

$$j = neU \tag{4.66}$$

So

$$n_i eU = n_i e\sqrt{\frac{kT}{M}}\left(1 - \frac{e\phi}{kT}\right) \tag{4.67}$$

$$U = \sqrt{\frac{kT}{M}}\left(1 - \frac{e\phi}{kT}\right) \tag{4.68}$$

$$U\sqrt{\frac{M}{kT}} = \left(1 - \frac{e\phi}{kT}\right) \tag{4.69}$$

$$\frac{e\phi}{kT} = 1 - U\sqrt{\frac{M}{kT}} \tag{4.70}$$

$$\phi = \frac{kT}{e}\left(1 - U\sqrt{\frac{M}{kT}}\right) \tag{4.71}$$

So putting in above equation

We get

$$\frac{\partial \nabla U}{\partial t} - \beta\frac{\partial U}{\partial x} - \gamma\frac{\partial^2 \nabla U}{\partial x^2} + \mu\frac{\partial^3 U}{\partial x^3} = 0 \tag{4.72}$$

Here

$$\gamma = \left(\frac{1}{n}\right)\sqrt{\frac{kT}{M}} \tag{4.73}$$

It is originated from the fact of overall charged neutrality condition of the plasmas.

We can present above equation in terms of stream function ψ to obtain the solution of this second order partial differential equation for the GRS environment.

$$\frac{\partial}{\partial t}(\nabla_{\perp}^{2}\psi) - \beta\frac{\partial \nabla_{\perp}\psi}{\partial x} - \gamma\frac{\partial^{2}}{\partial x^{2}}(\nabla_{\perp}^{2}\psi) + \mu\frac{\partial^{3}\nabla_{\perp}\psi}{\partial x^{3}} = 0 \tag{4.74}$$

Here

$$\nabla_{\perp}^{2} = \frac{\partial^{2}}{\partial x^{2}} + \frac{\partial^{2}}{\partial y^{2}} \tag{4.75}$$

It is the two-dimensional non-divergent viscous flow on an β-plane is the model used as a prototype implies precisely planetary atmospheric vortices.

Considering the parameters from the data base article (Wong et. al. 2021[22]) along with the dimensionless parameters are introduced as

$$(x, y) = L_0(x', y') \tag{4.76}$$

$$t = \frac{L_0 t'}{U_0} \tag{4.77}$$

$$\psi = L_0 U_0 \psi' \tag{4.78}$$

$$\beta = \frac{U_0 \beta'}{L_0^2} \tag{4.79}$$

Assuming the oscillatory solution

We get

$$\frac{\partial}{\partial t}(\nabla_{\perp}^{2}\psi) - \beta\frac{\partial \nabla_{\perp}\psi}{\partial x} - \gamma\frac{\partial^{2}}{\partial x^{2}}(\nabla_{\perp}^{2}\psi) + \mu\frac{\partial^{3}\nabla_{\perp}\psi}{\partial x^{3}} \sim \exp[\mathrm{i}((\boldsymbol{k}.\boldsymbol{r}) - \omega t)] \tag{4.81}$$

The dispersion relation of the linear wave can be obtained as,

$$\left(k_x + \frac{\beta}{2\omega}\right)^2 + k_y^2 - \gamma k_x^2 k_y^2 + \mu k_x^3 = \left(\frac{\beta}{2\omega}\right)^2 \tag{4.82}$$

This is the dispersion relation of the wave, which is known as the linear solution of rotating fluid and can reproduced well known Rossby wave if electrostatic force due to charged particle is ignored. The wave is exclusive to rotating fluids. The absence of this wave occurs when the sphere is not rotating.

4.1.5 Non-linear analysis

$$\frac{\partial \boldsymbol{u}}{\partial t} + (\boldsymbol{u}.\boldsymbol{\nabla})\boldsymbol{u} = \mu\nabla^{2}\boldsymbol{u} - \frac{\boldsymbol{\nabla}P}{\rho} - 2(\boldsymbol{\Omega}\times\boldsymbol{u}) + \frac{e}{\rho}\boldsymbol{\nabla}\phi - \chi(\mathbf{u}-\mathbf{v}) - \eta(\mathbf{u}-\mathbf{w}) \tag{4.83}$$

$(\boldsymbol{u}.\boldsymbol{\nabla})\boldsymbol{u}$, That is non-linear term so solving it

$$(\boldsymbol{u}.\boldsymbol{\nabla})\boldsymbol{u} = \left((U\hat{\boldsymbol{x}} + V\hat{\boldsymbol{y}}).\left(\frac{\partial}{\partial x}\hat{\boldsymbol{x}} + \frac{\partial}{\partial y}\hat{\boldsymbol{y}}\right)\right)(U\hat{\boldsymbol{x}} + V\hat{\boldsymbol{y}}) \tag{4.84}$$

$$(\boldsymbol{u}.\boldsymbol{\nabla})\boldsymbol{u} = \left(U\frac{\partial}{\partial x} + V\frac{\partial}{\partial y}\right)(U\hat{\boldsymbol{x}} + V\hat{\boldsymbol{y}}) \tag{4.85}$$

$$(\boldsymbol{u}.\boldsymbol{\nabla})\boldsymbol{u} = U\frac{\partial U}{\partial x}\hat{\boldsymbol{x}} + U\frac{\partial V}{\partial x}\hat{\boldsymbol{y}} + V\frac{\partial U}{\partial y}\hat{\boldsymbol{x}} + V\frac{\partial V}{\partial y}\hat{\boldsymbol{y}} \tag{4.86}$$

$$(\boldsymbol{u}.\boldsymbol{\nabla})\boldsymbol{u} = \left(U\frac{\partial U}{\partial x} + V\frac{\partial U}{\partial y}\right)\hat{\boldsymbol{x}} + \left(U\frac{\partial V}{\partial x} + V\frac{\partial V}{\partial y}\right)\hat{\boldsymbol{y}} \tag{4.87}$$

Now as

$$(\boldsymbol{u}.\boldsymbol{\nabla})\boldsymbol{u} = 0 \tag{4.88}$$

$$\boldsymbol{u} = U\hat{\boldsymbol{x}} + V\hat{\boldsymbol{y}} \tag{4.89}$$

$$U = \frac{\partial \psi}{\partial y} \tag{4.90}$$

$$V = -\frac{\partial \psi}{\partial x} \tag{4.91}$$

$$\boldsymbol{u} = \boldsymbol{\nabla}\psi \times \boldsymbol{z} \tag{4.92}$$

So putting values in Navier Stokes equation

We get

$$\frac{\partial \boldsymbol{u}}{\partial t} + (\boldsymbol{u}.\boldsymbol{\nabla})\boldsymbol{u} = \mu\nabla^2\boldsymbol{u} - \frac{\boldsymbol{\nabla}P}{\rho} - 2(\boldsymbol{\Omega} \times \boldsymbol{u}) + \frac{e}{\rho}\boldsymbol{\nabla}\phi - \chi(\mathbf{u} - \mathbf{v}) - \eta(\mathbf{u} - \mathbf{w}) \tag{4.93}$$

Here

$$2\boldsymbol{\Omega} = \Omega_x\hat{\boldsymbol{x}} + \Omega_y\hat{\boldsymbol{y}} \tag{4.94}$$

$$\Omega_x\hat{\boldsymbol{x}} = 0 \tag{4.95}$$

$$\Omega_y\hat{\boldsymbol{y}} = f(\hat{\boldsymbol{y}}) \tag{4.96}$$

$$2\boldsymbol{\Omega} = 0 + f(\hat{\boldsymbol{y}}) \tag{4.97}$$

$$2\boldsymbol{\Omega} = f(\hat{\boldsymbol{y}}) \tag{4.98}$$

Putting in above

$$\frac{\partial \boldsymbol{u}}{\partial t} + (\boldsymbol{u}.\boldsymbol{\nabla})\boldsymbol{u} = \mu\nabla^2\boldsymbol{u} - \frac{\boldsymbol{\nabla}P}{\rho} - 2(\boldsymbol{\Omega} \times \boldsymbol{u}) + \frac{e}{\rho}\boldsymbol{\nabla}\phi \tag{4.99}$$

$$\frac{\partial \boldsymbol{u}}{\partial t} + (\boldsymbol{u}.\boldsymbol{\nabla})\boldsymbol{u} + 2(\boldsymbol{\Omega} \times \boldsymbol{u}) = \mu\nabla^2\boldsymbol{u} - \frac{\boldsymbol{\nabla}P}{\rho} + \frac{e}{\rho}\boldsymbol{\nabla}\phi \tag{4.100}$$

$$\frac{\partial \boldsymbol{u}}{\partial t} + (\boldsymbol{u}.\boldsymbol{\nabla})\boldsymbol{u} + f(\hat{\boldsymbol{y}}) \times \boldsymbol{u} = \mu\nabla^2\boldsymbol{u} - \frac{\boldsymbol{\nabla}P}{\rho} + \frac{e}{\rho}\boldsymbol{\nabla}\phi \tag{4.101}$$

Putting

$$\boldsymbol{u} = \boldsymbol{\nabla}\psi \times \boldsymbol{z} \tag{4.102}$$

In above

$$\frac{\partial}{\partial t}(\boldsymbol{\nabla}\psi \times \boldsymbol{z}) + \big((\boldsymbol{\nabla}\psi \times \boldsymbol{z}).\boldsymbol{\nabla}\big)(\boldsymbol{\nabla}\psi \times \boldsymbol{z}) + f(\hat{\boldsymbol{y}}) \times (\boldsymbol{\nabla}\psi \times \boldsymbol{z}) = -\frac{\boldsymbol{\nabla}P}{\rho} + \mu\nabla^2(\boldsymbol{\nabla}\psi \times \boldsymbol{z}) + \frac{e}{\rho}\boldsymbol{\nabla}\phi \tag{4.103}$$

Taking curl on both sides

$$\boldsymbol{\nabla} \times \left(\frac{\partial}{\partial t}(\psi \times \boldsymbol{z}) + \big((\boldsymbol{\nabla}\psi \times \boldsymbol{z}).\boldsymbol{\nabla}\big)(\boldsymbol{\nabla}\psi \times \boldsymbol{z}) + f(\hat{\boldsymbol{y}}) \times (\boldsymbol{\nabla}\psi \times \boldsymbol{z})\right) = \boldsymbol{\nabla} \times \left(-\frac{\boldsymbol{\nabla}P}{\rho} + \mu\nabla^2(\boldsymbol{\nabla}\psi \times \boldsymbol{z}) + \frac{e}{\rho}\boldsymbol{\nabla}\phi\right) \tag{4.104}$$

$$\boldsymbol{\nabla} \times \frac{\partial}{\partial t}(\boldsymbol{\nabla}\psi \times \boldsymbol{z}) \tag{4.105}$$

$$\boldsymbol{\nabla} \times \big((\boldsymbol{\nabla}\psi \times \boldsymbol{z}).\boldsymbol{\nabla}\big)(\boldsymbol{\nabla}\psi \times \boldsymbol{z}) \tag{4.106}$$

$$\boldsymbol{\nabla} \times f(\hat{\boldsymbol{y}}) \times (\boldsymbol{\nabla}\psi \times \boldsymbol{z}) \tag{4.107}$$

$$\boldsymbol{\nabla} \times -\frac{\boldsymbol{\nabla}P}{\rho} \tag{4.108}$$

$$\boldsymbol{\nabla} \times \mu\nabla^2(\boldsymbol{\nabla}\psi \times \boldsymbol{z}) \tag{4.109}$$

$$\boldsymbol{\nabla} \times \frac{e}{\rho}\boldsymbol{\nabla}\phi \tag{4.110}$$

Solving equation (4.105)

$$\boldsymbol{\nabla} \times \frac{\partial}{\partial t}(\boldsymbol{\nabla}\psi \times \boldsymbol{z}) = \frac{\partial}{\partial t}\boldsymbol{\nabla} \times (\boldsymbol{\nabla}\psi \times \boldsymbol{z}) \tag{4.111}$$

$$\boldsymbol{\nabla}\psi \times \boldsymbol{z} = \begin{pmatrix} \hat{\boldsymbol{x}} & \hat{\boldsymbol{y}} & \hat{\boldsymbol{z}} \\ \frac{\partial \psi}{\partial x} & \frac{\partial \psi}{\partial y} & 0 \\ 0 & 0 & 1 \end{pmatrix} \tag{4.112}$$

$$\boldsymbol{\nabla}\psi \times \boldsymbol{z} = -\frac{\partial \psi}{\partial x}\hat{\boldsymbol{y}} + \frac{\partial \psi}{\partial y}\hat{\boldsymbol{x}} \tag{4.113}$$

Now

$$\boldsymbol{\nabla} \times (\boldsymbol{\nabla}\psi \times \boldsymbol{z}) = \begin{pmatrix} \hat{\boldsymbol{x}} & \hat{\boldsymbol{y}} & \hat{\boldsymbol{z}} \\ \frac{\partial}{\partial x} & \frac{\partial}{\partial y} & 0 \\ \frac{\partial \psi}{\partial y} & -\frac{\partial \psi}{\partial x} & 0 \end{pmatrix} \tag{4.114}$$

$$\boldsymbol{\nabla} \times (\boldsymbol{\nabla}\psi \times \boldsymbol{z}) = -\nabla^2\psi\hat{\boldsymbol{z}} \tag{4.115}$$

So

$$\boldsymbol{\nabla} \times \frac{\partial}{\partial t}(\boldsymbol{\nabla}\psi \times \boldsymbol{z}) = -\frac{\partial}{\partial t}\nabla^2\psi\hat{\boldsymbol{z}} \tag{4.116}$$

Solving equation (4.106)

$$\boldsymbol{\nabla} \times \big((\boldsymbol{\nabla}\psi \times \boldsymbol{z}).\boldsymbol{\nabla}\big)(\boldsymbol{\nabla}\psi \times \boldsymbol{z}) \tag{4.117}$$

From above

$$\boldsymbol{\nabla} \times (\boldsymbol{\nabla}\psi \times \boldsymbol{z}) = -\nabla^2\psi\hat{\boldsymbol{z}} \tag{4.118}$$

So

$$\boldsymbol{\nabla} \times \big((\boldsymbol{\nabla}\psi \times \boldsymbol{z}).\boldsymbol{\nabla}\big)(\boldsymbol{\nabla}\psi \times \boldsymbol{z}) = (\boldsymbol{\nabla}\psi \times \boldsymbol{z}).\boldsymbol{\nabla}(\nabla^2\psi) \tag{4.119}$$

Solving equation (4.107)

$$\boldsymbol{\nabla} \times f(\hat{\boldsymbol{y}}) \times (\boldsymbol{\nabla}\psi \times \boldsymbol{z}) = \boldsymbol{\nabla} \times f(\hat{\boldsymbol{y}}) \times \left(-\frac{\partial \psi}{\partial x}\hat{\boldsymbol{y}} + \frac{\partial \psi}{\partial y}\hat{\boldsymbol{x}}\right) \tag{4.120}$$

$$f(\hat{\boldsymbol{y}}) \times \left(-\frac{\partial \psi}{\partial x}y + \frac{\partial \psi}{\partial y}x\right) = \begin{pmatrix} \hat{\boldsymbol{x}} & \hat{\boldsymbol{y}} & \hat{\boldsymbol{z}} \\ 0 & 0 & f_o + \beta y \\ \frac{\partial \psi}{\partial y} & \frac{\partial \psi}{\partial x} & 0 \end{pmatrix} \tag{4.121}$$

$$f(\hat{\boldsymbol{y}}) \times \left(-\frac{\partial \psi}{\partial x}y + \frac{\partial \psi}{\partial y}x\right) = x(f_o + \beta y)\frac{\partial \psi}{\partial x} + y(f_o + \beta y)\frac{\partial \psi}{\partial y} \tag{4.122}$$

Now

$$\boldsymbol{\nabla} \times f(\hat{\boldsymbol{y}}) \times (\boldsymbol{\nabla}\psi \times \boldsymbol{z}) = \begin{pmatrix} \hat{\boldsymbol{x}} & \hat{\boldsymbol{y}} & \hat{\boldsymbol{z}} \\ \frac{\partial}{\partial x} & \frac{\partial}{\partial y} & 0 \\ f(y)\frac{\partial \psi}{\partial x} & f(y)\frac{\partial \psi}{\partial y} & 0 \end{pmatrix} \tag{4.123}$$

$$\boldsymbol{\nabla} \times f(\hat{\boldsymbol{y}}) \times (\boldsymbol{\nabla}\psi \times \boldsymbol{z}) = \hat{\boldsymbol{z}}\left(\frac{\partial}{\partial x}f(y)\frac{\partial \psi}{\partial y}\frac{\partial^2 \psi}{\partial x \partial y} - f(y)\frac{\partial^2 \psi}{\partial x \partial y} - \frac{\partial \psi}{\partial x}\left(\frac{\partial}{\partial y}\right)f(y)\right) \tag{4.124}$$

$$\boldsymbol{\nabla} \times f(\hat{\boldsymbol{y}}) \times (\boldsymbol{\nabla}\psi \times \boldsymbol{z}) = -\beta\frac{\partial \psi}{\partial x}\hat{\boldsymbol{z}} \tag{4.125}$$

Solving equation (4.108)

$$\boldsymbol{\nabla} \times -\frac{\boldsymbol{\nabla} P}{\rho} = -\frac{1}{\rho}\begin{pmatrix} \hat{\boldsymbol{x}} & \hat{\boldsymbol{y}} & \hat{\boldsymbol{z}} \\ \frac{\partial}{\partial x} & \frac{\partial}{\partial y} & \frac{\partial}{\partial z} \\ \frac{\partial P}{\partial x} & \frac{\partial P}{\partial y} & \frac{\partial P}{\partial z} \end{pmatrix} \tag{4.126}$$

$$\boldsymbol{\nabla} \times -\frac{\boldsymbol{\nabla} P}{\rho} = 0 \tag{4.127}$$

Solving equation (4.109)

$$\boldsymbol{\nabla} \times \mu \nabla^2 (\boldsymbol{\nabla}\psi \times \boldsymbol{z}) = \mu \boldsymbol{\nabla} \times \nabla^2 \left(-\frac{\partial \psi}{\partial x} \widehat{\boldsymbol{y}} + \frac{\partial \psi}{\partial y} \widehat{\boldsymbol{x}} \right) \tag{4.128}$$

$$\boldsymbol{\nabla} \times \mu \nabla^2 (\boldsymbol{\nabla}\psi \times \boldsymbol{z}) = \mu \nabla \times \left(\frac{\partial^2}{\partial x^2} + \frac{\partial^2}{\partial y^2} \right) \left(-\frac{\partial \psi}{\partial x} \widehat{\boldsymbol{y}} + \frac{\partial \psi}{\partial y} \widehat{\boldsymbol{x}} \right) \tag{4.129}$$

$$\boldsymbol{\nabla} \times \mu \nabla^2 (\boldsymbol{\nabla}\psi \times \boldsymbol{z}) = \mu \nabla \times \left(\left(\frac{\partial^3 \psi}{\partial x^2 \partial y} + \frac{\partial^3 \psi}{\partial y^3} \right) \widehat{\boldsymbol{x}} + \left(\frac{\partial^3 \psi}{\partial y^2 \partial x} + \frac{\partial^3 \psi}{\partial x^3} \right) \widehat{\boldsymbol{y}} \right) \tag{4.130}$$

$$\boldsymbol{\nabla} \times \mu \nabla^2 (\boldsymbol{\nabla}\psi \times \boldsymbol{z}) = \begin{pmatrix} \widehat{\boldsymbol{x}} & \widehat{\boldsymbol{y}} & \widehat{\boldsymbol{z}} \\ \frac{\partial}{\partial x} & \frac{\partial}{\partial y} & 0 \\ \frac{\partial^3 \psi}{\partial x^2 \partial y} + \frac{\partial^3 \psi}{\partial y^3} & \frac{\partial^3 \psi}{\partial y^2 \partial x} + \frac{\partial^3 \psi}{\partial x^3} & 0 \end{pmatrix} \tag{4.131}$$

By solving we get

$$\boldsymbol{\nabla} \times \mu \nabla^2 (\boldsymbol{\nabla}\psi \times \boldsymbol{z}) = 0 \tag{4.132}$$

Solving equation (4.110)

$$\boldsymbol{\nabla} \times \frac{e}{\rho} \boldsymbol{\nabla}\phi = \frac{e}{\rho} (\boldsymbol{\nabla} \times \boldsymbol{\nabla}\phi) \tag{4.133}$$

$$\boldsymbol{\nabla} \times \frac{e}{\rho} \boldsymbol{\nabla}\phi = \frac{e}{\rho} \begin{pmatrix} \widehat{\boldsymbol{x}} & \widehat{\boldsymbol{y}} & \widehat{\boldsymbol{z}} \\ \frac{\partial}{\partial x} & \frac{\partial}{\partial y} & 0 \\ \frac{\partial \phi}{\partial x} & \frac{\partial \phi}{\partial y} & 0 \end{pmatrix} \tag{4.134}$$

$$\boldsymbol{\nabla} \times \frac{e}{\rho} \boldsymbol{\nabla}\phi = 0 \tag{4.135}$$

Putting above values

$$-\frac{\partial}{\partial t}\nabla^2\psi + ((\boldsymbol{\nabla}\psi \times \boldsymbol{z}).\boldsymbol{\nabla}(\nabla^2\psi)) - \beta\left(\frac{\partial\psi}{\partial x}\right) = 0 \tag{4.136}$$

$$\frac{\partial}{\partial t}\nabla^2\psi + ((\boldsymbol{\nabla}\psi \times \boldsymbol{z}).\boldsymbol{\nabla}(\nabla^2\psi)) + \beta\left(\frac{\partial\psi}{\partial x}\right) = 0 \tag{4.137}$$

A class of two-dimensional flow has been taken into account in this work. The Charney—Hasegawa—Mima equation, in which the vorticity is proportional to the stream function (Shivamoggi, 1989 [44]), appears to be analogous to above Eq. (4.137)

Chapter 5: Results and Discussion

We have done linear as well as non-linear analysis. In linear analysis we can see from equations that we have effects like viscosity, corlious and electric potential. On the other hand during non-linear analysis we have effects like viscosity and corlious force effect. Large-scale atmospheric waves, such as Rossby waves, might behave similarly in both longitudinal and latitudinal directions due to the planets' rapid rotation and resulting zonal (east-west) symmetry. However, certain factors like differential rotation rates and varying latitudinal temperature gradients could introduce some differences. Wave amplitude refers to the magnitude or height of the waves in a fluid system, such as the atmosphere of a gaseous giant. It is a measure of the strength or intensity of the wave. Rossby wave describe that wave amplitude follows similar laws in both x y direction.

Identifying propagating waves from the mathematical solution is challenging. However, by looking at the manner in which wave number one's symmetries change on a basic-state velocity profile, the wave mechanics may still be comprehended. Wave number one (k=1) corresponds to the fundamental mode of a wave. In spherical harmonics, it represents the longest wavelength wave that can fit around the circumference of the planet. This wave has a simple structure, often showing clear, large-scale patterns in the atmosphere. Symmetries refer to the repeating patterns in the wave structure. These symmetries can change depending on the underlying flow conditions, such as the basic-state velocity profile. The basic-state velocity profile is the background flow of the atmosphere, often represented by the average zonal (east-west) wind speeds as a function of latitude and height.

Relative Vorticity Map:

Relative Vorticity: Vorticity is a measure of the local rotation in a fluid flow. The relative vorticity specifically refers to the vorticity relative to the rotating reference frame of the planet.

Mean Absolute Value: The average magnitude of this vorticity is $\sim 10^{-5} s^{-1}$ in the outer region of the vortex over the timeline considered. So vorticity is local rotation within fluid. We can find vorticity by taking curl of the stream function that is being defined in equations.

Velocity Fields:

Scattered-Vector Velocity Fields: These are velocity measurements at scattered points, possibly derived from observations or calculations.

Gridded Velocity Field: This is a velocity field that has been interpolated onto a regular grid, making it easier to analyze and visualize.

Cuts through Principal Axes of the Vortex: This refers to analyzing the velocity field by taking cross-sectional views along the main axes (usually the major and minor axes) of the vortex.

Data Source:

The data for these analyses comes from observations made with the WFC3/UVIS (Wide Field Camera 3 / Ultraviolet-Visible) instrument on the Hubble Space Telescope (HST), as reported by Dressel (2021 [23]).

Parameters Used:

Mean Absolute Value of Relative Vorticity: $\sim 10^{-5} s^{-1}$ in the outer region.

High-Speed Ring: Refers to the faster-moving outer part of the vortex.

Length Scales:

Zonal Length Scale (L_x):L_x $\sim 10^6$km. This is the horizontal scale of the vortex along the direction of the planet's rotation (longitude).

Meridional Length Scale (L_y): L_y $\sim 10^5$km. This is the horizontal scale of the vortex perpendicular to the direction of the planet's rotation (latitude). As we know that we have to consider imaginary curves around planet to define latitude and longitude and during this we find out that latitudes curves are being parallel to each other while curves of longitude are perpendicular to each other.

Atmospheric and Planetary Parameters:

Atmosphere Height (H): H $\sim 10^2$km. This is the vertical scale of the atmosphere where the vortex is located.

Gravity (g): g=24.79 m/s^2. This is the gravitational acceleration on Jupiter.

Characteristic Length and Velocity:

Zonal Characteristic Length (L_o): ~10^6km. This is a representative horizontal scale for the vortex structure in the zonal direction.

Characteristic Zonal Velocity Scale (U_0): This value is derived from the available data, indicating a typical speed of the fluid motion in the zonal direction. The exact value is not provided here but is obtained from onboard data (Wong et al., 2021) [22].

The relative vorticity map shows average vorticity values in the outer region of the GRS, while different velocity fields (scattered-vector, gridded, and cross-sectional cuts) provide detailed insights into the flow patterns within the vortex.

Numerical Solution of Eq. (4.74):

Characteristic Length and Velocity Scales: The characteristic length corresponds to the radius of maximum winds (RMW), and the velocity scale corresponds to the maximum tangential velocity.

Reference: The data and parameters used are based on Wong et al. (2021) [22].

Rossby Solution Method:

The numerical solution is obtained using the Rossby solution method, as described by Liu et al. (2018). This method is used to analyze wave motions in rotating fluids. From our results if we ignore the electric potential then we will get the linear solution as rossby wave. So electric potential is important to be considered here as there will be charge produced on dust particles.

Visualization (Fig. 5.1):

Contour Plot (Left): Displays the relationship between longitude, latitude, and stream functions at a zonal velocity scale $U_0 = 120\ m/sec$.

3D Plot (Right): Provides a three-dimensional view of the same parameters, offering a more detailed perspective on the vortex structure.

Rayleigh's Stability Condition:

The vortex satisfies Rayleigh's necessary condition for exponential stability, indicating that the mean vorticity is a monotonic function of radius. This criterion ensures that the vortex is stable and will not undergo exponential growth or decay (Gent and McWilliams, 1986[45]).

Validation of Conclusions:

The conclusions are validated for various swirl solutions with finite energy and angular momentum. Despite the vortex containing integrated kinetic energy and angular momentum, the solutions remain consistent.

Wave Propagation:

Outward-Propagating Waves: These waves have length scales smaller than the typical radial scale L_0 of the vortex. The numerical results show that these waves move outward from the center of the vortex.

Behavior of Solution: Fig. 5.1 illustrates outward-propagating wave packets, revealing three important characteristics:

Expansion of Packets: Individual wave packets expand quickly as they move outward from the center of the vortex. As in the core we see that vorticity is high while on the other hand we see that as we move from core to the surrounding of the vortex vorticity decreases.

Non-Monotonic Stream Function: The stream function, which describes the flow of the fluid, exhibits a non-monotonic behavior, indicating complex variations in the flow pattern.

Wave Dispersion: The group velocity, which is the speed at which the overall shape of the wave packets moves, shows dispersion. This means that different wavelengths travel at different speeds, affecting the shape and behavior of the wave packets over time.

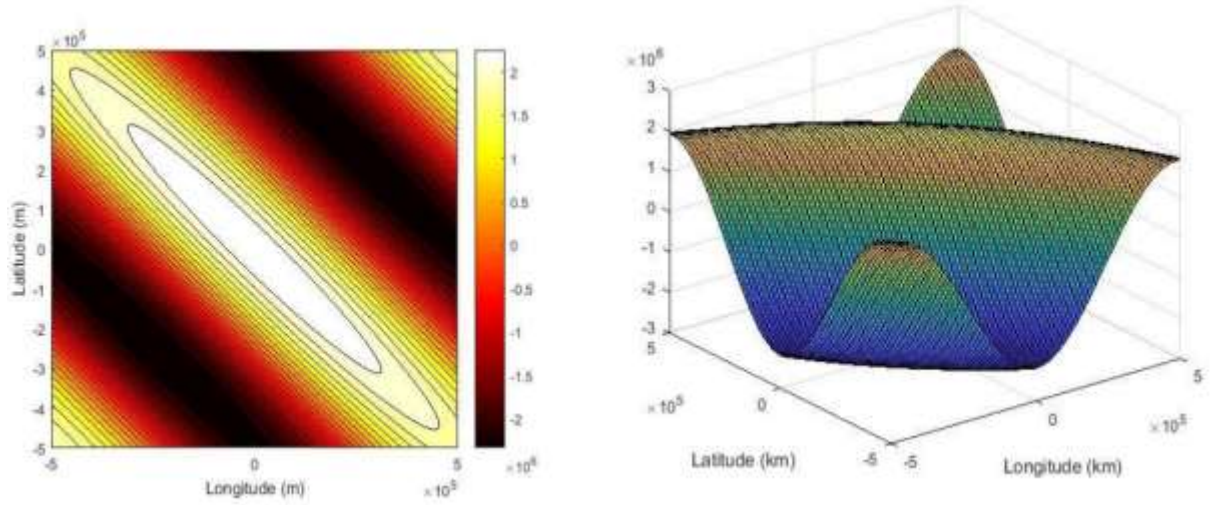

Figure 5.1 : Relationship between longitude, latitude, and stream functions

From equation (4.82)

Stable Vortex-Flows and Energy Exchange:

In a stable vortex flow, disturbances (or waves) can transfer energy from one part of the vortex to another. This process is crucial for understanding how energy is distributed and maintained within the vortex. So we can define the stability of vortex based on the energy exchange process. As we have seen that when there is high energy in one part of the vortex then there is low energy on the other part and due to this energy will flow from high part to low part of vortex.

Wave Dispersion and Fig. 5.2:

Wave Dispersion: Describes how waves of different wavelengths (or wavenumbers) travel at different speeds within the vortex.

Fig. 5.2: Shows the relationship between the frequency of oscillation ω and the wavenumbers k_x(on the left) k_y(on the right).

Dispersion Relation Eq. (4.82):

This equation relates the frequency ω of the waves to their wavenumbers k_x andk_y. Where $k_x = 2\pi/L_0$and$k_y = 2\pi/L_0$. It is used to determine the stability and behavior of the waves in the vortex.

Roots of Eq. (4.82): The solutions (roots) of this equation indicate the presence of stable or unstable modes. In this case, no imaginary roots are found, indicating the absence of unstable modes and hence confirming the stability of the vortex.

Wave Frequency and Wavenumbers:

Frequency as a Function of k_x : On the left side of Fig. 5.2, the frequency decreases with increasingk_x.

Frequency as a Function of k_y: On the right side of Fig. 5.2, the frequency increases with increasingk_y.

This variation supports the energy exchange process mentioned earlier, where energy is transferred across different wavenumber bands.

Monotonic Trends and Stability:

The frequency of the modes changes monotonically with wavenumber, indicating a regular and predictable behavior without any instabilities.

The absence of imaginary roots in the dispersion relation confirms the stability of the vortex against dissipative mechanisms.

Influence of Kinematic Viscosity:

Kinematic Viscosity: This is a measure of a fluid's resistance to flow and deformation. Three different values of kinematic viscosity are considered: $10^7 m^2/sec$, $2 \times 10^7 m^2/sec$ and $5 \times 10^7 m^2/sec$ (Vidmachenko, 1986 [36]).

Effect on Frequency: As kinematic viscosity increases, the frequency of the waves decreases for a given wavenumber. This is depicted in Fig. 5.2 with solid red, dotted black, and dashed blue curves.

Electrostatic Effect:

The electrostatic effect is not considered in this analysis$\phi \to 0$, simplifying the third term in Eq. (133)

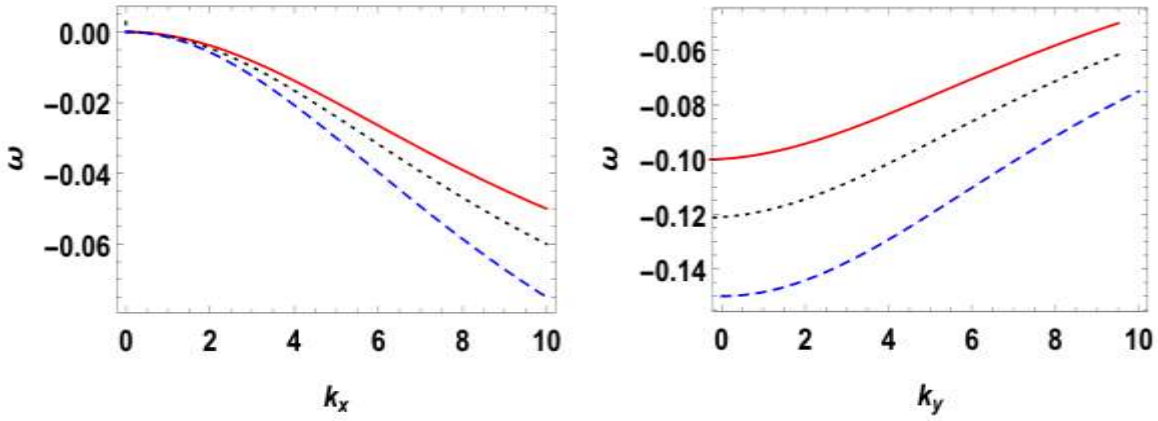

Figure 5.2 : Relationship between the frequency of oscillation ω and the wavenumbers (on the left) (on the right)

Finite Electrostatic Effect on Wave Propagation:

The inclusion of the electrostatic effect significantly influences the linear wave dynamics in the vortex. This is an additional factor that modifies the behavior of the waves, beyond the effects of vorticity and viscosity. So electric potential has played vital role in the dynamics of vortex as we can see from results.

Fig. 5.3 Description:

Electrostatic Parameter (γ): Represents the influence of electrostatic effects on the wave dynamics. Three different values are considered, $\gamma = 0.1$, $\gamma = 0.2$ and $\gamma = 0.3$.

Curves in Fig. 5.3:

Solid Red Curve: Corresponds to $\gamma = 0.1$.

Dotted Black Curve: Corresponds to $\gamma = 0.2$.

Dashed Blue Curve: Corresponds to $\gamma = 0.3$.

Effect of γ on Wave Frequency:

Increased Frequency: As the concentration of plasma particles (represented by γ) increases, the frequency of the waves also increases for a given wavenumber. This means that the waves oscillate faster when there are more plasma particles present.

Propagation at Lower k_x and k_y : The waves propagate more readily at lower values of the wavenumbers k_x and k_y . This implies that the influence of the electrostatic effect allow the waves to propagate over larger scales in the zonal and meridional directions.

Introducing the parameter γ to account for electrostatic effects reveals that plasma particle concentration significantly impacts wave dynamics. With higher γ values, the frequency of the waves increases, indicating faster oscillations. The waves can propagate at lower wavenumbers (k_x and k_y), meaning they can travel over larger scales in both the longitudinal (zonal) and latitudinal (meridional) directions. By considering electrostatic effects, researchers can better understand the full range of factors that influence wave dynamics in the GRS. This includes the role of charged particles and plasma within Jupiter's atmosphere. Including γ in numerical model helps refine predictions and improve the accuracy of simulations related to wave propagation and

vortex stability. This analysis reveals the significant role of electrostatic effects in altering wave dynamics of the GRS and sheds new light on the sustenance mechanisms of these massive vortices.

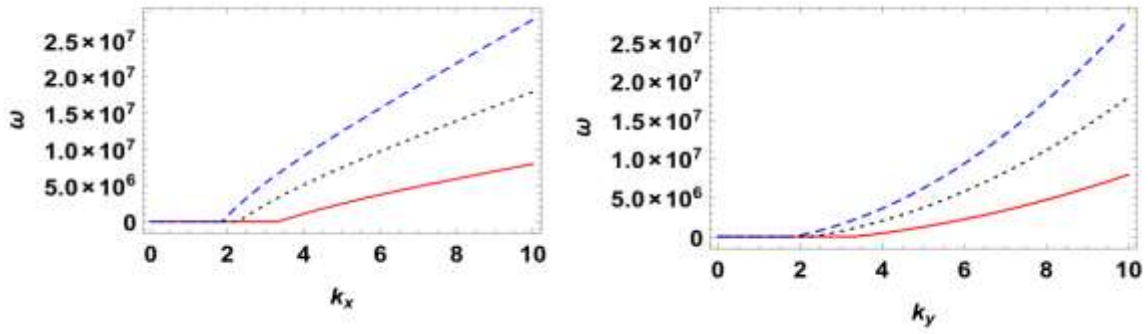

Figure 5.3 : Relationship between the frequency of oscillation ω and the wavenumbers (on the left) (on the right)

Analytical Dispersion Relation (Eq. 4.82):

This relation describes how the frequency of wave modes varies with respect to the wavenumbers k_x and k_y .

Parametric Analysis: The dispersion relation has been evaluated through a parametric analysis, where different values of k_x and k_y are considered to understand their effects on the mode frequency.

Numerical Solution and Frequency Spectrum:

A numerical solution is obtained for the frequency of the mode, giving a detailed frequency spectrum as a function of k_x and k_y .

Fig. 5.4: This figure presents the frequency spectrum in three dimensions, illustrating how the mode frequency varies with k_x and k_y . Basically it's a counter paragraph that shows that how wave is propagating at different frequency in longitude and in latitude which are shown by wave numbers.

Ranges of k_x and k_y :

The analysis considers $0 \leq k_x, k_y \leq 10$, covering a range from zero to the maximum wavenumber.

Equal Contribution of Wave Frequency: At $k_x = k_y = 10$, the wave vectors propagating in mutually perpendicular directions contribute equally to the mode frequency.

Stable Oscillations:

Range for Stability: Stable oscillations are found within the range $2 \leq k_x \leq 4 \; and \; 2 \leq k_y \leq 4$.

Island of Oscillation: This term refers to the specific region in the k_x-k_y space where stable, linear oscillations occur, indicating a stable structure for the rotating wave.

Fig. 5.4 provides a 3D visualization of how the mode frequency changes with k_x and k_y, offering insights into the dynamics of the waves. At the maximum wavenumbers $k_x = k_y = 10$the wave vectors in perpendicular directions contribute equally to the mode frequency. The stable oscillations are found within the specific range of k_x and k_y, , identifying a region (an "island") where the waves maintain a stable, linear structure.

We can also see that at lower wave numbers wave is travelling in one direction only so we can compare this region to our results where we have ignore the electric potential. And in higher wave numbers we can see that the wave is propagating in both directions so its means that we can compare this to the effects where electric potential are being added. And in between we see that there is a stable region named as island of oscillations where we see that waves are oscillating within a define region where there are stable oscillation because we can see that at there we have minima so at minima we know that system energy is in stable environment. So we can say that vortex has a dynamics in such a way that its energy is transferring from one part to other part and due to this flow there is exchange process that is occurring due to which the vortex maintain its shape.

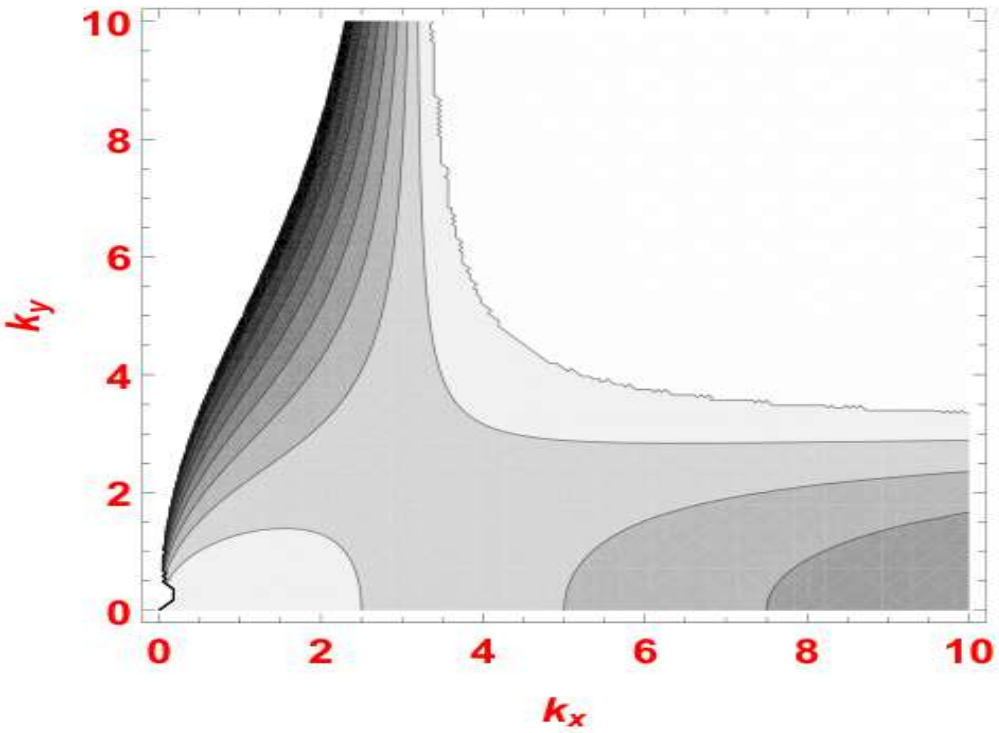

Figure 5.4 : Frequency modes variation with kx and ky

From Equation (4.137).

Using parameters describing above with appropriate boundary conditions (Simon *et. al.*, 2014 [10]; Rogers, 2008 [15]) and vorticity sources relevant to the confined GRS's vortex, the steady-state solutions of Eq. (4.137) are depicted in Fig. 5.

Parameters and Boundary Conditions:

Circular Domain: A circular domain with an aspect ratio $L_y/L_x = 0.5$ is used to model the GRS, that is appropriate to the GRS's current display size as specified in Rogers, 2008[15].

Zonal Jets: The GRS is modeled as a quasi-steady circulation within stable zonal jets, which have a weak eastward peak at 26.5° S and a westward peak at 19.5° S. This could

potentially be the cause of the GRS's horizontal drift in a westward direction (Rogers, 2008).

Steady-State Solutions and Streamline Patterns (Fig. 5.5):

Contours of ψ: The left side of Fig. 5.5 shows the contours of the stream function ψ, illustrating the steady-state dust flow streamline patterns.

Corresponding Structure: The right side shows the corresponding structure in the latitude/longitude plane.

Vorticity Distribution: At a specific viscosity regime (Vidmachenko, 1986 [36]), the vorticity along the boundary is symmetric, uniformly diffuse, and relatively weak.

Flow Dynamics:

Circulation and Vorticity: The related streamline pattern is a circulation that follows the geometry of the confined GRS as illustrated. The dynamical changes have a relatively minimal impact on viscosity and are related to vorticities and zonal flow velocities. The dynamical regime, not the geometry of the confined domain, determines the state of the flow that retains more momentum or energy, and as a result, the flow structure changes rather slowly. Instead of diffusing directly towards the outer region, the vorticity close to the boundary can convict along the streamlines and then dissipate inside the vortex because of the relative increase in convective transport. The streamline pattern follows the geometry of the confined GRS. Vorticity near the boundary convicts along the streamlines and dissipates inside the vortex due to increased convective transport.

Self-Organized State: The subsequent streamline patterns are circular and they transform into a new self-organized state with a circular core region surrounded by high speed collar layers that separate the core from the regions around it filled with thin and prolonged vortices. So we can say that within vortex these stream lines flow in a particular direction that is circular and as we move from core to boundary of the vortex these stream line then convert their shape to the surrounding environment shape of stream line.

Velocity Profiles and Wind Shear:

Cross-Section Profiles: Cross-section profiles of velocity *U* passing through the center of the circulation (x_0, y_0) against latitude are used to illustrate the structural changes at vorticity in the 10^{-1} to 10^{-6} s^{-1} range (top left is 10^{-1} to bottom right 10^{-6}) of the bounded dust flow in Fig. 5.

Mean Wind Shear: We examined the mean wind shear (Wong et al., 2021 [22]) spanning the 20–25°S region in order to rule out the possibility that changes in the GRS velocity field were caused by changes in the vortex surrounds. The average wind speed in the high-speed ring and long-term variations in vortex size, shape, and wind shear do not show a monotonic shift in the wind shear. **Rossby Number**: The non-dimensional Rossby number $R_0 = U_0/f_0L_0$ is the relation between the strength of the inertial and Coriolis forces. We observed that the GRS's Rossby number did not correspond to long-term patterns. Because shear in the environment of vortices produces deviations from circular shape (e.g., Marcus, 1990 [37]; Moore & Saffman, 1971 [38]), a decrease in the amount of the anticyclonic shear in the surrounding flow could explain a long-term change in aspect ratio.

Environmental Shear and Vortex Shape:

Deviations from Circular Shape: Shear in the environment can cause deviations from a circular shape. A decrease in anticyclonic shear could explain long-term changes in the aspect ratio of the GRS.

Wind Shear Trends: Over the period 2009 to 2020, the environmental wind shear did not decrease. It is unclear whether the wind shear is increasing with time (which, in the absence of any other factors, would lengthen rather than circularize the GRS), or whether it changes in a more complex manner.

This analysis provides a comprehensive view of the steady-state dynamics of the Great Red Spot, highlighting the intricate interplay between vorticity, flow patterns, and environmental shear. The findings contribute to our understanding of the stability and evolution of atmospheric vortices, offering valuable insights for future research.

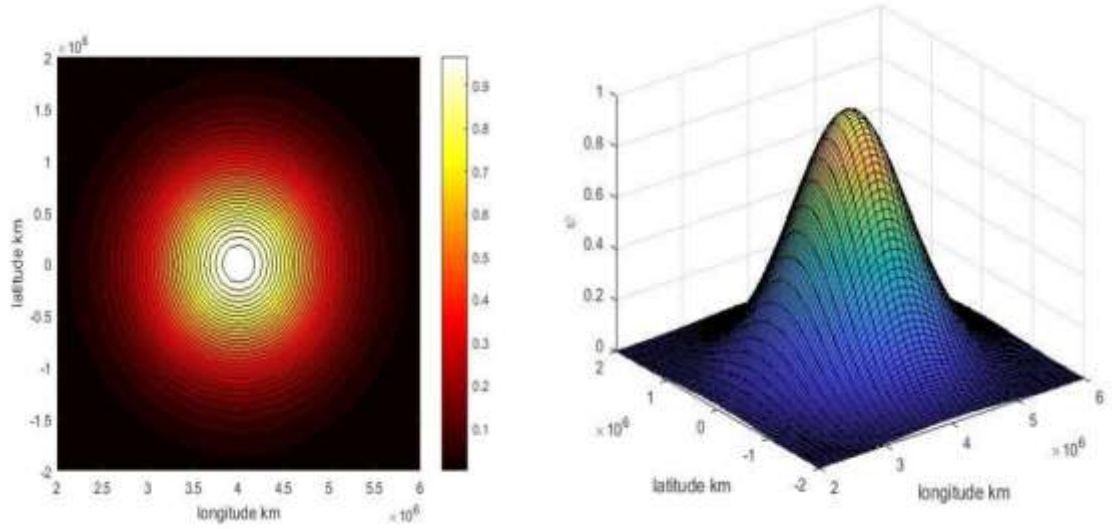

Figure 5.5 : Contours of the stream function ψ (left) and corresponding structure in the Latitude /longitude plane (right)

Vorticity Analysis:

Profile Shape and Decay Factors: The vorticity in the outer region of the GRS is examined in relation to the profile shape of the velocity field across the high-speed ring. The term "decay factors" refers to how quickly the velocity decreases from the center of the vortex outward.

Ruling Out Prolonged Changes in Static Stability: The study intends to ascertain long-term static stability changes in the GRS by examining vorticity's impact on the velocity profile. The resistance of the atmosphere to vertical displacement determines static stability.

Velocity Profile and Vortices:

Amplitude of Velocity Profile: For lower vorticity levels, an amplified velocity profile emerges. With lower vorticity, the peak velocities in the flow profile increase.

Fig. 5.6: Fig. 5.6 depicts the probable relationship between vorticity and velocity profile amplitude.

Altitude Coverage:

Horizontal Wind Fields: The wind fields in the study focus on a limited altitude range. The findings only apply to specific layers of the GRS's atmosphere.

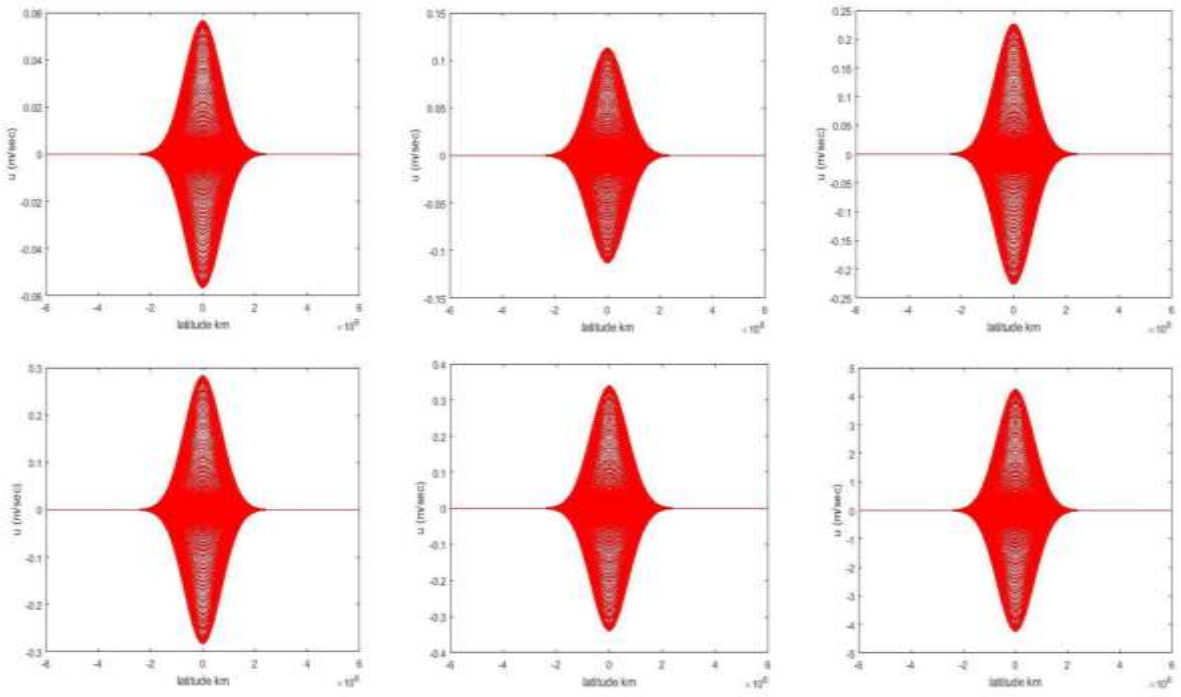

Figure 5.6 : Relationship between vorticity and the amplitude of the velocity profile

Development of a New Mathematical Model:

The mathematical model proposed here aims to explain Jupiter's atmospheric vortices' structure, stability, and shape theoretically. This model aims to represent the fundamental movements of vortices, unattainable through mere observational data alone. The mathematical model was designed to capture the structural, stable, and morphological features of vortex dynamics. This model aims to represent the fundamental aspects of vortex formation, development, and structure preservation. The model deals with vortex dynamics, addressing their movement, stability, and morphological transformations. A new mathematical model signifies a crucial progression in the field, serving as a theoretical

counterpart to observational models. An in-depth comprehension of vortex dynamics may result in more precise forecasts of their behavior.

Comparison with Existing Models:

Jupiter's atmospheric static stability predictions in vortex models largely depend on imaging and wind field data. These models accurately depict atmospheric features and dynamics through direct observation.

Existing vortex models heavily rely on imaging and wind field data. Jupiter's atmospheric features and wind patterns are mapped using observational data from spacecraft and telescopes.

The widely-used models for predicting Jupiter's atmospheric static stability are these ones. Understanding the planet's dynamics and weather patterns relies on assessing the atmosphere's resistance to vertical motions, known as static stability.

The study by Brueshaber and Sayanagi referenced in the passage focuses on modeling vortex dynamics using observational data. [38] A study by Brueshaber et al. points to ongoing investigation in this field. [39] For decades, modeling vortex dynamics using imaging and wind field data has been a prevalent approach. [41, 42]

Chapter 6: Conclusions and Recommendations

The theoretical model we proposed is designed to interpret the turbulence behaviors observed in the vortex on Jupiter and Saturn, accurately representing the particle dynamics that occur in the planet's real atmosphere. One significant limitation of this model is that it uses a two-dimensional (2D) framework, even though the actual dynamics of these vortices are three-dimensional (3D) and influenced by internal processes (as discussed by Ingersoll et al., 2000 [28]). Despite this, our linear analysis reveals wave dispersion, demonstrating how waves interact within these vortices.

In stable vortex flows, the impact of kinematic viscosity is minimal, indicating that it doesn't significantly alter the behavior of the vortices. Both linear and nonlinear solutions from our model show an essential wave process where disturbances can remove energy from the vortex at one frequency band and deposit it at another. This energy transfer is crucial for understanding how vortices maintain their structure and dynamics over time.

Zonal jets' shear features significantly influence the size, power, and orientation of atmospheric vortices within planetary bands. The Coriolis force, a result of a planet's rapid rotation, influences vortices by altering their absolute vorticity. The collective impact of these factors implies that streaming zonal jets are the primary influencers of vortex formation and behavior on Jupiter and Saturn.

The dynamics of Jupiter's GRS vortices are primarily influenced by alterations in zonal jet properties, driving fields, and vorticity. Kinematic viscosity has a smaller impact compared to dynamic viscosity. Understanding these vortices' defining traits becomes clearer with this newfound insight.

6.1 Recommendations for Further Work

By integrating theoretical and observational techniques, researchers can gain a more comprehensive grasp of gas giants' atmospheres, vital for predicting their weather and dynamics. Theoretical models offer insight into the fundamental physics behind vortex dynamics, which includes wave dispersion, energy transfer, and the impacts of zonal jets and the Coriolis force.

These models aid in uncovering the underlying mechanisms responsible for the development, change, and persistence of vortices such as the Great Red Spot.

Observational data from instruments like imaging devices and wind field sensors prove the occurrence of these processes. Real-time atmospheric phenomena on Jupiter are captured by this data, providing intricate understandings of vortices and other dynamic characteristics. Through the combination of theoretical models and observational data, researchers establish precise representations of gas giant atmospheric vortices.

By integrating both methods, the analysis becomes more robust, accurate, and reliable in regards to vortex dynamics and stability predictions. Theoretical models can be validated through comparison with observational data regarding vortex behavior under specific conditions. Discrepancies can refine the models. Through iterative model validation and refinement, atmospheric phenomena are better understood, leading to improved planetary weather forecasts.

References

[1] P. Murad, "An Investigation of the Prehistory Cosmology of the Solar System."

[2] G. Sbaiz, "Some stability and instability issues in the dynamics of highly rotating fluids," *arXiv preprint arXiv:2205.11889*, 2022.

[3] T. Owen and D. Gautier, "Touring the saturnian system: the atmospheres of titan and saturn," *Space science reviews*, vol. 104, no. 1, pp. 347-376, 2002.

[4] "Hubble Tracks Jupiter's Stormy Weather." https://science.nasa.gov/missions/hubble/hubble-tracks-jupiters-stormy-weather/ (accessed.

[5] L. F. Smith, J. K. Smith, K. K. Arcand, R. K. Smith, and J. A. Bookbinder, "Aesthetics and Astronomy: How Museum Labels Affect the Understanding and Appreciation of Deep-Space Images," *Curator: The Museum Journal*, vol. 58, no. 3, pp. 282-297, 2015.

[6] "Saturn's Rings Shine in New Hubble Portrait." https://hubblesite.org/contents/news-releases/2019/news-2019-43 (accessed.

[7] F. F. Chen, *Introduction to plasma physics*. Springer Science & Business Media, 2012.

[8] P. S. Marcus, "Jupiter's Great Red Spot and other vortices," *In: Annual review of astronomy and astrophysics. Vol. 31 (A94-12726 02-90), p. 523-573.*, vol. 31, pp. 523-573, 1993.

[9] A. R. Vasavada *et al.*, "Galileo imaging of Jupiter's atmosphere: The Great Red Spot, equatorial region, and white ovals," *Icarus*, vol. 135, no. 1, pp. 265-275, 1998.

[10] A. A. Simon *et al.*, "Dramatic change in Jupiter's Great Red Spot from spacecraft observations," *The Astrophysical Journal Letters*, vol. 797, no. 2, p. L31, 2014.

[11] D. S. Choi, A. P. Showman, and A. R. Vasavada, "The evolving flow of Jupiter's White Ovals and adjacent cyclones," *Icarus*, vol. 207, no. 1, pp. 359-372, 2010.

[12] P. S. Marcus and S. Shetty, "Jupiter's zonal winds: are they bands of homogenized potential vorticity organized as a monotonic staircase?," *Philosophical Transactions of the Royal Society A: Mathematical, Physical and Engineering Sciences*, vol. 369, no. 1937, pp. 771-795, 2011.

[13] A. A. Simon, F. Tabataba-Vakili, R. Cosentino, R. F. Beebe, M. H. Wong, and G. S. Orton, "Historical and contemporary trends in the size, drift, and color of Jupiter's great red spot," *The Astronomical Journal*, vol. 155, no. 4, p. 151, 2018.

[14] J. L. Mitchell, R. F. Beebe, A. P. Ingersoll, and G. W. Garneau, "Flow fields within Jupiter's Great Red Spot and white oval BC," *Journal of Geophysical Research: Space Physics*, vol. 86, no. A10, pp. 8751-8757, 1981.

[15] J. H. Rogers, "The accelerating circulation of Jupiter's Great Red Spot," *Journal of the British Astronomical Association, vol. 118, no. 1, p. 14-20*, vol. 118, pp. 14-20, 2008.

[16] A. A. Simon-Miller *et al.*, "New observational results concerning Jupiter's great red spot," *Icarus*, vol. 158, no. 1, pp. 249-266, 2002.

[17] B. Sun, C. Liu, and F. Wang, "Global meridional eddy heat transport inferred from Argo and altimetry observations," *Scientific Reports*, vol. 9, no. 1, p. 1345, 2019.

[18] R. Hueso *et al.*, "Saturn atmospheric dynamics one year after Cassini: Long-lived features and time variations in the drift of the Hexagon," *Icarus*, vol. 336, p. 113429, 2020.

[19] K. M. Sayanagi *et al.*, "Dynamics of Saturn's great storm of 2010–2011 from Cassini ISS and RPWS," *Icarus*, vol. 223, no. 1, pp. 460-478, 2013.

[20] P. S. Marcus, "Prediction of a global climate change on Jupiter," *Nature*, vol. 428, no. 6985, pp. 828-831, 2004.

[21] A. Simon, "Outer Planet Atmospheres Legacy (" OPAL")," *MAST, doi,* vol. 10, no. 17909, p. T9G593, 2015.
[22] M. H. Wong, P. S. Marcus, A. A. Simon, I. de Pater, J. W. Tollefson, and X. Asay-Davis, "Evolution of the horizontal winds in Jupiter's Great Red Spot from one Jovian year of HST/WFC3 maps," *Geophysical Research Letters,* vol. 48, no. 18, p. e2021GL093982, 2021.
[23] L. Dressel, "Wide Field Camera 3 Instrument Handbook for Cycle 29, v13. 0 (Baltimore MD: STScI)," ed, 2021.
[24] X. S. Asay-Davis, P. S. Marcus, M. H. Wong, and I. De Pater, "Jupiter's shrinking Great Red Spot and steady Oval BA: Velocity measurements with the 'Advection Corrected Correlation Image Velocimetry'automated cloud-tracking method," *Icarus,* vol. 203, no. 1, pp. 164-188, 2009.
[25] "Advection Corrected Correlation Image Velocimetry (ACCIV)." https://github.com/xylar/acciv (accessed.
[26] P. S. Marcus and C. Lee, "Jupiter's Great Red Spot and zonal winds as a self-consistent, one-layer, quasigeostrophic flow," *Chaos: An Interdisciplinary Journal of Nonlinear Science,* vol. 4, no. 2, pp. 269-286, 1994.
[27] T. E. Dowling and A. P. Ingersoll, "Jupiter's Great Red Spot as a shallow water system," *Journal of Atmospheric Sciences,* vol. 46, no. 21, pp. 3256-3278, 1989.
[28] A. Ingersoll, P. Gierasch, D. Banfield, A. Vasavada, and f. Galileo Imaging Team, "Moist convection as an energy source for the large-scale motions in Jupiter's atmosphere," *Nature,* vol. 403, no. 6770, pp. 630-632, 2000.
[29] M. J. Loeffler, R. L. Hudson, N. J. Chanover, and A. A. Simon, "The spectrum of Jupiter's Great Red Spot: The case for ammonium hydrosulfide (NH4SH)," *Icarus,* vol. 271, pp. 265-268, 2016.
[30] S. Weidenschilling and J. Lewis, "Atmospheric and cloud structures of the Jovian planets," *Icarus,* vol. 20, no. 4, pp. 465-476, 1973.
[31] B. B. Kadomtsev and V. I. Petviashvili, "On the stability of solitary waves in weakly dispersing media," in *Doklady Akademii Nauk,* 1970, vol. 192, no. 4: Russian Academy of Sciences, pp. 753-756.
[32] M. Groves and S.-M. Sun, "Fully localised solitary-wave solutions of the three-dimensional gravity–capillary water-wave problem," *Archive for rational mechanics and analysis,* vol. 188, pp. 1-91, 2008.
[33] E. I. a. G. Rowlands, *Nonlinear Waves, Solitons and Chaos*. 2000.
[34] V. Zakharov and E. Kuznetsov, "On three dimensional solitons," *Zhurnal Eksp. Teoret. Fiz,* vol. 66, pp. 594-597, 1974.
[35] T. A. Guinn and W. H. Schubert, "Hurricane spiral bands," *Journal of the atmospheric sciences,* vol. 50, no. 20, pp. 3380-3403, 1993.
[36] A. Vidmachenko, "Some dynamical parameters of the atmosphere of Jupiter," *Kinematics and Physics of Celestial Bodies,* vol. 2, no. 1, pp. 54-56, 1986.
[37] P. S. Marcus, "Vortex dynamics in a shearing zonal flow," *Journal of Fluid Mechanics,* vol. 215, pp. 393-430, 1990.
[38] D. Moore and P. G. Saffman, "Structure of a line vortex in an imposed strain," in *Aircraft Wake Turbulence and Its Detection: Proceedings of a Symposium on Aircraft Wake Turbulence held in Seattle, Washington, September 1–3, 1970. Sponsored jointly by the*

Flight Sciences Laboratory, Boeing Scientific Research Laboratories and the Air Force Office of Scientific Research, 1971: Springer, pp. 339-354.

[39] S. R. Brueshaber and K. M. Sayanagi, "Effects of forcing scale and intensity on the emergence and maintenance of polar vortices on Saturn and Ice Giants," *Icarus,* vol. 361, p. 114386, 2021.

[40] S. R. Brueshaber, K. M. Sayanagi, and T. E. Dowling, "Dynamical regimes of giant planet polar vortices," *Icarus,* vol. 323, pp. 46-61, 2019.

[41] J. Y. K. Cho, M. de la Torre Juárez, A. P. Ingersoll, and D. G. Dritschel, "A high-resolution, three-dimensional model of Jupiter's Great Red Spot," *Journal of Geophysical Research: Planets,* vol. 106, no. E3, pp. 5099-5105, 2001.

[42] S. Shetty and P. S. Marcus, "Changes in Jupiter's great red spot (1979–2006) and oval Ba (2000–2006)," *Icarus,* vol. 210, no. 1, pp. 182-201, 2010.

[43] A. Barkan, N. D'angelo, and R. L. Merlino, "Charging of dust grains in a plasma," *Physical Review Letters,* vol. 73, no. 23, p. 3093, 1994.

[44] B. K. Shivamoggi, "Charney-hasegawa-mima equation: A general class of exact solutions," *Physics Letters A,* vol. 138, no. 1-2, pp. 37-42, 1989.

[45] P. R. Gent and J. C. McWilliams, "The instability of barotropic circular vortices," *Geophysical & Astrophysical Fluid Dynamics,* vol. 35, no. 1-4, pp. 209-233, 1986.